28415-H009-R0-00

CR 151855

ENGINEERING DESCRIPTION OF THE OMS/RCS/DAP MODELS USED IN THE HP-9825A HIGH FIDELITY RELATIVE MOTION PROGRAM (HFRMP)

(NASA-CR-151855) ENGINEERING DESCRIPTION OF THE OMS/RCS/DAP MODES USED IN THE HP-9825A HIGH FIDELITY RELATIVE MOTION PROGRAM (HFRMP) (TRW Defense and Space Systems Group) 77 p HC A05/MF A01 CSCL 22A G3/16

N79-12137

Unclas 38895

6 OCTOBER 1978

PREPARED FOR

NATIONAL AERONAUTICS AND SPACE ADMINISTRATION

LYNDON B. JOHNSON SPACE CENTER

CONTRACT NAS 9-~~14273~~ 14723

SYSTEMS ENGINEERING AND ANALYSIS DEPARTMENT

TRW

DEFENSE AND SPACE SYSTEMS GROUP

HOUSTON, TEXAS

28415-H009-R0-00

ENGINEERING DESCRIPTION OF THE OMS/RCS/DAP MODELS USED IN THE HP-9825A HIGH FIDELITY RELATIVE MOTION PROGRAM (HFRMP)

6 OCTOBER 1978

Prepared for

NATIONAL AERONAUTICS AND SPACE ADMINISTRATION
LYNDON B. JOHNSON SPACE CENTER

Contract NAS 9-14273

Prepared by S. W. Wilson

S. W. Wilson, Manager
Shuttle/IUS Proximity
Operations Software Project

Approved D. K. Phillips

D. K. Phillips, Manager
Systems Engineering and
Analysis Department

Systems Engineering and Analysis Department

TRW
DEFENSE AND SPACE SYSTEMS GROUP

Houston, Texas

ABSTRACT

This report describes simplified mathematical models of the Space Shuttle's Orbital Maneuvering System (OMS), Reaction Control System (RCS), and on-orbit Digital Autopilot (DAP) that have been incorporated in the High-Fidelity Relative Motion Program (HFRMP) for the HP-9825A desk-top calculator. Comparisons are made between data generated by the HFRMP and by the Space Shuttle Functional Simulator (SSFS), which models the cited Shuttle systems in much greater detail. These data include propellant requirements for representative translational maneuvers, rotational maneuvers, and attitude maintenance options. Also included are data relating to on-orbit trajectory deviations induced by RCS translational cross coupling. Potential close-range stationkeeping problems that are suggested by HFRMP simulations of 80 millisecond (as opposed to 40 millisecond) DAP cycle effects are described. The principal function of the HFRMP is to serve as a flight design tool in the area of proximity operations. However, the simplified models it uses may be of value in other applications, for instance in ground-based orbit determination (navigational) calculations.

TABLE OF CONTENTS

LIST OF TABLES

LIST OF FIGURES

SYMBOLS AND ACRONYMS

$\bar{a}$	Linear acceleration vector
a	Magnitude or component of linear acceleration
C	DAP cycle time
C	RCS jet torque factor (Table 1)
CG	Center of gravity
D	Attitude deadband width
D	Drift mode
DAP	Digital Autopilot
$\bar{F}$	Force vector
F	Magnitude or component of force
FULL	Full cross coupling compensation
HFRMP	High Fidelity Relative Motion Program
[I]	Inertia tensor
I	Element of inertia tensor
IRH	Inertial rate hold
I_{SP}	Specific impulse
$\bar{L}$	Torque vector
L	Magnitude or component of torque
LV	Local vertical
LVRH	Local vertical rate hold
MLD	Geocentric inertial Mean of Launch Date reference frame
M50	Geocentric inertial Mean of 1950.0 reference frame
OMS	Orbital Maneuvering System
P	Primary (Reaction Control System)
PLV	Payload-centered local vertical reference frame
POP	Perpendicular to the orbit plane
PRCS	Primary Reaction Control System
PZI	Primary (Reaction Control System) with +Z jets inhibited
$\bar{\bar{q}}$	Unit quaternion
$\tilde{\tilde{q}}$	Conjugate of unit quaternion
$\bar{R}$	Position of RCS thrust application point relative to CG
RCS	Reaction Control System

ROT	Rotational cross coupling compensation
SBY	Shuttle (Orbiter) body axes reference frame
SLV	Shuttle-centered local vertical reference frame
STA,BL,WL	Orbiter station coordinates (corresponding to X_0, Y_0, Z_0 in the Orbiter structural body frame)
SSFS	Space Shuttle Functional Simulator
t	Time
T	RCS electrical pulse width
T*	RCS effective pulse width
V	Vernier (Reaction Control System)
VRCS	Vernier Reaction Control System
W	Weight
$\dot{W}$	Propellant consumption rate
X,Y,Z	Orthogonal Cartesian axes (Orbiter body axes unless otherwise identified)
ZLV	Orbiter Z axis aligned continuously with local vertical direction
$\overline{\alpha}$	Angular acceleration vector produced by control jets
α	Magnitude or component of $\overline{\alpha}$
α	Control jets opposing ν, or the angular acceleration component magnitude they produce
β	Control jets reinforcing ν, or the angular acceleration component magnitude they produce
θ	Angular displacement (error)
ν	Magnitude of angular acceleration component produced by natural torques and inertial effects
τ	Interval between RCS control pulses
ω	Angular velocity, $\dot{\theta}$

1. INTRODUCTION

The HP-9825A High Fidelity Relative Motion Program (HFRMP) is a 12-degrees-of-freedom trajectory integrator (6 degrees of freedom for each of two vehicles) which generates digital and graphical data to describe the relative motion of the Space Shuttle Orbiter and a free-flying payload. These data are obtained by differencing the geocentric states of the individual vehicles, computed to a numerical precision of 12 decimal digits, with respect to an oblate earth whose gravitational model includes the second harmonic coefficient (J_2). The state of the two-vehicle system is computed as a function of time by means of a fourth-order Runge-Kutta numerical integration scheme which uses quaternions to define both the rotational and the translational states of each vehicle (Reference 1).

The payload is modeled geometrically as a cylinder whose length and diameter are specified by program input. The Orbiter and the payload are treated as rigid bodies whose individual mass properties (gross weight, moments and products of inertia, and center of gravity location) are specified by program input and are assumed to remain constant[†] during the HFRMP run. Gravity gradient torque is included in the rotational equations of motion for both vehicles. At the user's option, aerodynamic torque and drag can also be included for either or both vehicles. Aerodynamic forces normal to the relative wind vector are ignored.

The atmosphere is assumed to rotate with the earth, and is modeled as a function of geodetic altitude by a curve fit of the 1962 Standard density profile (Reference 2). The density profile can be modified by a program input factor to account for the major effects of solar activity. Aerodynamic drag and moment coefficients for the Orbiter are computed as curve-fit functions of its attitude with respect to the relative wind vector (References 3-5).

[†]An exception is made when integrating the trajectory of an upper stage during a major translational maneuver such as an IUS solid rocket motor burn. In such a case, the payload gross weight is decremented during the burn to reflect the consumption of propellant.

Aerodynamically, the payload is modeled as a flat plate whose size and shape are determined by projecting its cylindrical outline onto a plane normal to the relative wind vector. The payload drag coefficient is assumed to be 2.0, based on its projected frontal area. Aerodynamic effects on the Orbiter and the payload can be modified (or cancelled entirely) by means of input factors which are applied uniformly to all aerodynamic forces and torques that are computed for the specified vehicle.

Several options are provided for defining the initial state of the two-vehicle system. The translational state of the Orbiter can be described either in terms of osculating orbit elements referenced to the Mean of 1950.0 (M50) geocentric equatorial frame, or in terms of invariant orbit elements (Reference 6) measured in the Mean of Launch Date (MLD) equatorial frame. The initial attitude of the Orbiter is defined by pitch, yaw, and roll angles (taken in that order) referenced to the rotating Shuttle-centered local-vertical (SLV) coordinate system. The Orbiter's angular velocity, measured in terms of rate components about its body axes, can be defined relative to either the M50 (inertial) frame or the SLV (rotating) frame.

The initial translational state of the payload is defined by rectangular position and velocity components which are measured relative to the Orbiter's center of gravity (CG). At the user's option, these components can be measured in the SLV coordinate system, or in the Shuttle body (SBY) coordinate system. The payload's initial pitch, yaw, and roll angles can be referenced either to the payload-centered local-vertical (PLV) system, or to the SBY system. The payload's angular rate components about its body axes can be defined relative to the M50, the PLV, or the SBY frame.

The initial state of the system can be advanced through up to 40 flight profile segments, each of arbitrary length, which are defined by the user at the beginning of the HFRMP run.† At the beginning of any segment the user may

†All input data, including the flight profile definition, are saved in disk files whence they can be recalled (and edited, if necessary) for use in subsequent runs.

command the application of an impulsive (i.e., instantaneous) increment to the angular rate of either or both vehicles.[†] In this regard, the user may specify a particular rate increment (INCR), a desired rate with respect to inertial space (IR), or a desired rate with respect to the local-vertical frame of the vehicle in question (LVR). In all cases, the components of the desired rate or rate increment are measured about the body axes of the vehicle in question.

After applying the specified angular velocity increment (if any) at the beginning of the flight segment, the HFRMP then (for each vehicle independently of the other)

1. allows the attitude to drift (D) under the influence of inertia and natural torques, or
2. performs inertial rate hold (IRH) control (i.e., maintains a constant angular velocity relative to inertial space), or
3. performs local-vertical rate hold (LVRH) control (i.e., maintains a constant angular velocity relative to the rotating local-vertical frame of the vehicle being controlled)

for the duration of the segment, depending on the user's specifications for that segment.

When the IRH or the LVRH attitude-maintenance option is specified for the Orbiter, a simplified RCS/DAP model is used to compute average values for the propellant consumption rates and translational cross-coupling accelerations that result from the intermittent thruster firings which are required to apply the necessary control torques. The model takes into account the mass properties of the Orbiter, the electrical width (an integer multiple of the DAP cycle time) and the effective width (the duration of steady-state acceleration) of the RCS thruster pulses, and the width of the attitude deadband about each of the Orbiter's

---

[†]Commanded angular velocity impulses, and the linear velocity impulses which they may induce as a result of RCS translational cross coupling, are the only types of state variable discontinuity that are permitted by the HFRMP. These are allowed only at the beginning of a flight profile segment.

body axes. Deadbands can be changed from segment to segment in the flight profile, as can the selection of primary or vernier thrusters and the mode of cross-coupling compensation. Translational cross-coupling accelerations are integrated along with those produced by gravity, aerodynamics, and commanded translational thrust. They are reflected in the output data by the flight path deviations they produce. Propellant consumption rates are also integrated (but not subtracted from the Orbiter gross weight), and the accumulated expenditures are tabulated, along with other data, a user-specified time intervals. Propellant consumption is broken down according to source (forward, aft left, or aft right tank) and function (translational or rotational control).

When the IRH or the LVRH attitude-maintenance option is specified for the payload, the magnitudes of the necessary control torques are integrated and the accumulated rotational impulse (measured in pound-foot-seconds) in the positive and negative direction about each body axis is printed along with the other digital output data. Since no specific method of implementation is modeled, it is not possible to compute propellant consumption rates or cross-coupling effects that may result from payload attitude control.

Translational thrust acceleration of either or both vehicles can be commanded at the beginning of any flight profile segment. Payload translational thrust is always applied in the direction of the payload's +X body axis and is assumed to be directed through the CG. Once initiated, payload thrust acceleration continues until all of the rocket motor propellant is consumed, as determined by a table of flow rates versus burn time.

Translational acceleration of the Orbiter is initiated by commanding ignition of either or both of the OMS engines (L, R, or L+R) and/or by firing primary RCS thrusters to produce thrust nominally in the positive or negative directions of the Orbiter body axes (+X, -X, +Y, -Y, +Z, or -Z). Once initiated, Orbiter translational acceleration is applied continuously at the nominal steady-state level, throughout the duration of the flight profile segment. Detailed descriptions of the OMS and RCS models are contained in Sections 2 and 3.

2. OMS MODEL

The thrust vectors of the OMS engines are assumed always to pass through their respective gimbal centers (STA 1518, BL $\pm$ 88, WL 492) as defined by Reference 7 in terms of Orbiter station coordinates. When a single-engine OMS burn is commanded, the specified engine is gimbaled to direct its thrust vector through the Orbiter CG. When both engines are commanded to fire, they are gimbaled such that their two thrust vectors will be parallel and have moment arms about the CG of equal magnitude and opposite direction. Thus, in all cases, the OMS engines produce zero net torque.

Throughout the total duration of any flight profile segment in which it is commanded to fire, each OMS engine is assumed to deliver its nominal steady-state thrust magnitude of 6000 pounds, and to consume propellant at its nominal rate of 19.16 pounds/second (Reference 7). Flow rates are integrated and the accumulated propellant expenditure is listed separately for each engine in the HFRMP output data. However, the propellant expenditure is not subtracted from the Orbiter's gross weight. Therefore, this simplified model will not generate accurate data for a very large OMS burn where the propellant expenditure represents a significant fraction of the Orbiter gross weight.

3. RCS MODEL

Table 1 contains the basic data which are used to compute forces and torques produced by individual RCS jets. Each row in the table contains data for a particular jet. The first column on the left contains index numbers which are used internally by the HFRMP. The second column contains the jet identification mnemonics which are defined in Reference 7. The next three columns contain steady-state thrust components parallel to the Orbiter body axes. These are followed by three columns which contain the station coordinates of a thrust application point (i.e., a point on the jet's line of action). These coordinates are used, in conjunction with the quantity in the last column, to calculate torque about the Orbiter CG.

The data in Table 1 were derived from those shown in Tables 2 and 3, which are reproduced from References 7 and 8. The thrust components in Table 1 represent a summation of the basic thrust components from Table 2 and the incremental thrust components (due to plume impingement on Orbiter surfaces) from Table 3. For each jet listed in Table 3, the thrust application point coordinates in Table 1 were obtained by the following procedure:

1. Using the force components and application points from Table 2, a basic force moment vector was calculated about the reference CG location (STA 1076.7, BL 0, WL 374.1) which is associated with Table 3.

2. The torque increment due to impingement (from Table 3) was added to the torque calculated in step 1.

3. The resultant torque vector was resolved into two components; one parallel to the total force vector (columns 3-5 of Table 1), and the other normal to the total force vector.

4. The parallel torque component was divided by the magnitude of the total force vector. The result, which has the dimensions of feet, appears in the rightmost column of Table 1.

5. A line of action (effective thrust line) was calculated for the total force vector such that its moment about the reference CG was equal to the normal component of the total torque vector. The station coordinates of the new thrust application point (columns 6-8 of Table 1) represent the point on the calculated thrust line that is closest to the thrust application point originally designated in Table 2.

ORIGINAL PAGE IS
OF POOR QUALITY

Table 1. RCS Thruster Data

THRUSTER NO.	THRUSTER ID	F_X (LB)	F_Y (LB)	F_Z (LB)	STA (IN)	BL (IN)	WL (IN)	C (FT)
1	F2F	-879.4	-26.2	119.9	306.72	14.65	392.96	0.0000
2	F3F	-879.5	0.0	122.7	306.72	0.00	394.45	0.0000
3	F1F	-879.4	26.2	119.9	306.72	-14.65	392.96	0.0000
4	F1L	-26.3	873.6	18.2	362.67	-69.50	373.73	0.0000
5	F3L	-21.0	870.3	0.5	364.71	-71.65	359.25	0.0000
6	F2R	-26.3	-873.6	18.2	362.67	69.50	373.73	0.0000
7	F4R	-21.0	-870.3	0.5	364.71	71.65	359.25	0.0000
8	F2U	-32.3	-11.7	874.4	350.93	14.39	413.46	0.0000
9	F3U	-31.9	0.0	873.5	350.92	0.00	414.53	0.0000
10	F1U	-32.3	11.7	874.4	350.93	-14.39	413.46	0.0000
11	F2D	-28.0	-616.4	-639.5	333.84	61.42	356.95	0.0000
12	F1D	-28.0	616.4	-639.5	333.84	-61.42	356.95	0.0000
13	F4D	-24.8	-612.6	-639.4	348.44	66.23	358.44	0.0000
14	F3D	-24.8	612.6	-639.4	348.44	-66.23	358.44	0.0000
15	R3A	856.8	0.0	151.1	1555.29	137.00	473.06	0.0000
16	R1A	856.8	0.0	151.1	1555.29	124.00	473.06	0.0000
17	L3A	856.8	0.0	151.1	1555.29	-137.00	473.06	0.0000
18	L1A	856.8	0.0	151.1	1555.29	-124.00	473.06	0.0000
19	L4L	0.0	870.5	-8.4	1516.06	-149.83	455.21	-0.5887
20	L2L	0.0	870.5	-8.4	1529.07	-149.83	455.21	-0.6061
21	L3L	0.0	870.5	-8.4	1542.07	-149.83	455.21	-0.6235
22	L1L	0.0	870.5	-8.4	1555.07	-149.83	455.21	-0.6410
23	R4R	0.0	-870.5	-8.4	1516.06	149.83	455.21	0.5887
24	R2R	0.0	-870.5	-8.4	1529.07	149.83	455.21	0.6061
25	R3R	0.0	-870.5	-8.4	1542.07	149.83	455.21	0.6235
26	R1R	0.0	-870.5	-8.4	1555.07	149.83	455.21	0.6410
27	L4U	29.0	72.0	870.0	1520.04	-116.51	481.65	-0.4615
28	L2U	29.0	72.0	870.0	1532.96	-116.54	481.65	-0.3725
29	L1U	29.0	72.0	870.0	1545.87	-116.58	481.65	-0.2836
30	R4U	29.0	-72.0	870.0	1520.04	116.51	481.65	0.4615
31	R2U	29.0	-72.0	870.0	1532.96	116.54	481.65	0.3725
32	R1U	29.0	-72.0	870.0	1545.87	116.58	481.65	0.2836
33	L4D	312.4	346.8	-545.7	1498.11	-101.47	420.49	1.7413
34	L2D	312.4	346.8	-545.7	1513.68	-100.61	424.63	1.4807
35	L3D	312.4	346.8	-545.7	1529.23	-99.79	428.76	1.2208
36	R4D	312.4	-346.8	-545.7	1498.11	101.47	420.49	-1.7413
37	R2D	312.4	-346.8	-545.7	1513.68	100.61	424.63	-1.4807
38	R3D	312.4	-346.8	-545.7	1529.23	99.79	428.76	-1.2208
39	F5R	-0.8	-17.0	-17.6	324.35	59.70	350.12	0.0000
40	F5L	-0.8	17.0	-17.6	324.35	-59.70	350.12	0.0000
41	R5R	0.0	-24.0	-0.6	1565.00	149.87	459.00	0.0000
42	L5L	0.0	24.0	-0.6	1565.00	-149.87	459.00	0.0000
43	R5D	0.0	0.0	-24.0	1565.00	118.00	455.44	0.0000
44	L5D	0.0	0.0	-24.0	1565.00	-118.00	455.44	0.0000

Table 2. Basic RCS Thrust Data
(Without Plume Impingement)

THRUSTER ID	THRUST COMPONENTS, LB			RESULTANT THRUST, LB	STATION COORDINATES OF THRUST APPLICATION POINT (IN)		
	F_x	F_y	F_z		STA	BL	WL
F2F	-879.4	-26.2	119.9	887.9	306.72	14.65	392.96
F3F	-879.5	0.0	122.7	888.0	306.72	0.0	394.45
F1F	-879.4	26.2	119.9	887.9	306.72	-14.65	392.96
F1L	-26.3	873.6	18.2	874.2	362.67	-69.50	373.73
F3L	-21.0	870.3	0.5	870.6	364.71	-71.65	359.25
F2R	-26.3	-873.6	18.2	874.2	362.67	69.50	373.73
F4R	-21.0	-870.3	0.5	870.6	364.71	71.65	359.25
F2U	-32.3	-11.7	874.4	875.1	350.93	14.39	413.46
F3U	-31.9	0.0	873.5	874.1	350.92	0.0	414.53
F1U	-32.3	11.7	874.4	875.1	350.93	-14.39	413.46
F2D	-28.0	-616.4	-639.5	888.6	333.84	61.42	356.95
F1D	-28.0	616.4	-639.5	888.6	333.84	-61.42	356.95
F4D	-24.8	-612.6	-639.4	885.9	348.44	66.23	358.44
F3D	-24.8	612.6	-639.4	885.9	348.44	-66.23	358.44
F5R	-0.8	-17.0	-17.6	24.5	324.35	59.70	350.12
F5L	-0.8	17.0	-17.6	24.5	324.35	-59.70	350.12
R3A	856.8	0.0	151.1	870.0	1555.29	137.00	473.06
R1A	856.8	0.0	151.1	870.0	1555.29	124.00	473.06
L3A	856.8	0.0	151.1	870.0	1555.29	-137.00	473.06
L1A	856.8	0.0	151.1	870.0	1555.29	-124.00	473.06
L4L	0.0	870.5	-22.4	870.8	1516.00	-149.87	459.00
L2L	0.0	870.5	-22.4	870.8	1529.00	-149.87	459.00
L3L	0.0	870.5	-22.4	870.8	1542.00	-149.87	459.00
L1L	0.0	870.5	-22.4	870.8	1555.00	-149.87	459.00
R4R	0.0	-870.5	-22.4	870.8	1516.00	149.87	459.00
R2R	0.0	-870.5	-22.4	870.8	1529.00	149.87	459.00
R3R	0.0	-870.5	-22.4	870.8	1542.00	149.87	459.00
R1R	0.0	-870.5	-22.4	870.8	1555.00	149.87	459.00
L4U	0.0	0.0	870.0	870.0	1516.00	-132.00	480.50
L2U	0.0	0.0	870.0	870.0	1529.00	-132.00	480.50
L1U	0.0	0.0	870.0	870.0	1542.00	-132.00	480.50
R4U	0.0	0.0	870.0	870.0	1516.00	132.00	480.50
R2U	0.0	0.0	870.0	870.0	1529.00	132.00	480.50
R1U	0.0	0.0	870.0	870.0	1542.00	132.00	480.50
L4D	170.4	291.8	-801.7	870.0	1516.00	-111.95	437.40
L2D	170.4	291.8	-801.7	870.0	1529.00	-111.00	440.00
L3D	170.4	291.8	-801.7	870.0	1542.00	-110.06	442.60
R4D	170.4	-291.8	-801.7	870.0	1516.00	111.95	437.40
R2D	170.4	-291.8	-801.7	870.0	1529.00	111.00	440.00
R3D	170.4	-291.8	-801.7	870.0	1542.00	110.06	442.60
L5D	0.0	0.0	-24.0	24.0	1565.00	-118.00	455.44
R5D	0.0	0.0	-24.0	24.0	1565.00	118.00	455.44
L5L	0.0	24.0	-0.6	24.0	1565.00	-149.87	459.00
R5R	0.0	-24.0	-0.6	24.0	1565.00	149.87	459.00

(Reproduced from Reference 7)

Table 3. Force and Moment Increments Due to Plume Impingement (CG @ STA 1076.7, BL 0, WL 374.1)

THRUSTER ID	Δ FORCE (LB)			Δ MOMENT (LB-FT)		
	F_x	F_y	F_z	L_x	L_y	L_z
L4L			14	-450		
L2L			14	-450		
L3L			14	-450		
L1L			14	-450		
L4U	29	72		1755		-2780
L2U	29	72		1755		-2780
L1U	29	72		1755		-2780
L4D	142	55	256	-2520	10,480	-1395
L2D	142	55	256	-2520	10,480	-1395
L3D	142	55	256	-2520	10,480	-1395
R4R			14	450		
R2R			14	450		
R3R			14	450		
R1R			14	450		
R4U	29	-72		-1755		2780
R2U	29	-72		-1755		2780
R1U	29	-72		-1755		2780
R4D	142	-55	256	2520	10,480	1395
R2D	142	-55	256	2520	10,480	1395
R3D	142	-55	256	2520	10,480	1395

(Reproduced from Reference 8)

For a CG location defined by arbitrary station coordinates (STA_{cg}, BL_{cg}, WL_{cg}), the torque produced by a particular jet j is computed from the equation

$$\overline{L}_j = \overline{R}_j \times \overline{F}_j + C_j \overline{F}_j \quad , \tag{1}$$

where

$$\overline{F}_j = \begin{bmatrix} F_{xj} \\ F_{yj} \\ F_{zj} \end{bmatrix} \quad , \tag{2}$$

$$\overline{R}_j = \begin{bmatrix} -(STA_j - STA_{cg})/12 \\ (BL_j - BL_{cg})/12 \\ -(WL_j - WL_{cg})/12 \end{bmatrix} \quad , \tag{3}$$

and where the values of F_{xj}, F_{yj}, F_{zj}, STA_j, BL_j, WL_j, and C_j are obtained from columns 3-9 of Table 1.

4. DAP MODEL

4.1 JET SELECT TABLES

For each flight profile segment, the HFRMP user must specify which one of three basic combinations of thrusters is to be used for attitude and/or RCS translational control of the Orbiter. The available options are designated V (vernier jets), P (primary jets), and PZI (primary jets with +Z thrusters inhibited). Corresponding to each of those options is a jet-select table (Tables 4-6) which identifies the particular jet or combination of jets that is to be fired in response to each of the six possible translational acceleration commands (+X, -X, +Y, -Y, +Z, -Z) and the six possible rotational acceleration commands (+ROL, -ROL, +PCH, -PCH, +YAW, -YAW). Jets are identified by the mnemonics listed in the second column of Table 1. The jet select tables are not routinely available for modification by the user. However, an editing routine is available in the HFRMP software system, and changes can be made (or additional options can be provided) with little difficulty.

As indicated in Table 4 by the absence of any jet designations for the execution of translational acceleration commands, the V option (vernier jets) can be used only for attitude control. The P option (Table 5) and the PZI option (Table 6) can be used for translational and/or rotational control.

In the PZI option, no jets are fired that would expel propellant directly upward with respect to the Orbiter body. Translational acceleration in the downward direction, if commanded, is achieved (at a comparatively high propellant cost) by firing the +X and -X thrusters simultaneously. The cant angles of the +X jet and -X jet thrust lines produce a small net acceleration in the +Z (downward) direction. This option normally is used only when the Orbiter is maneuvering in the near vicinity of a payload that must be protected from jet plume impingement.

4.2 RESPONSE MATRICES

During HFRMP trajectory integration, steady-state accelerations and propellant consumption rates that result from RCS translational and rotational control commands are obtained from a pre-calculated "response matrix". As

Table 4. Vernier (V) Jet Select Table

CMD	THRUSTERS TO BE FIRED							
	1	2	3	4	5	6	7	8
+X								
-X								
+Y								
-Y								
+Z								
-Z								
+ROL	L5D							
-ROL	R5D							
+PCH	F5R	F5L						
-PCH	L5D	R5D						
+YAW	R5R							
-YAW	L5L							

ORIGINAL PAGE IS
OF POOR QUALITY

Table 5. Primary (P) Jet Select Table

CMD	THRUSTERS TO BE FIRED							
	1	2	3	4	5	6	7	8
+X	R1A	L1A						
-X	F2F	F1F						
+Y	F1L	L4L						
-Y	F2R	R4R						
+Z	F3U	L4U	R4U					
-Z	F1D	F2D	L4D	L2D	R4D	R2D		
+ROL	L4D	R4U						
-ROL	L4U	R4D						
+PCH	F1D	F2D	L4U	R4U				
-PCH	F3U	L4D	R4D					
+YAW	F1L	R4R						
-YAW	F2R	L4L						

Table 6. Primary with +Z Thrusters Inhibited (PZI) Jet Select Table

CMD	THRUSTERS TO BE FIRED							
	1	2	3	4	5	6	7	8
+X	R1A	L1A						
−X	F2F	F1F						
+Y	F1L	L4L						
−Y	F2R	R4R						
+Z	F2F	F1F	R1A	L1A				
−Z	F1D	F2D	L4D	L2D	R4D	R2D		
+ROL	L4D							
−ROL	R4D							
+PCH	F1D	F2D						
−PCH	L4D	R4D						
+YAW	F1L	R4R						
−YAW	F2R	L4L						

indicated in Tables 7-14 for a typical set of Orbiter mass properties which are listed in Table 15, the response to a particular command is conditioned by the jet select table (V, P, or PZI), and it is further conditioned by the user-specified mode of cross-coupling compensation. The available compensation modes are NONE (no compensation), ROT (rotational compensation only), and FULL (rotational and translational compensation).

The FULL compensation mode is not applicable when the vernier jets are selected;† therefore, eight different response matrices are sufficient to support all of the Orbiter control options that are currently provided in the HFRMP. Only one of these eight matrices is required to support trajectory integration in a given flight profile segment. All eight matrices are stored in disk files prior to the initiation of trajectory integration, and the appropriate one is read into calculator memory at the beginning of each segment. All eight matrices are re-calculated whenever the user makes any kind of change to the Shuttle Data Base (where the Orbiter mass properties are stored).

The response matrices are 12 x 12 arrays of real numbers. In a given matrix, each row corresponds to a particular translational or rotational control command.†† The first three columns of each matrix contain the body-axis components of the steady-state linear acceleration vector, and columns 4-6 contain the corresponding components of angular acceleration. Columns 7-9 contain rates of flow from the forward, aft left, and aft right tanks (in that order), for propellant consumption that is chargeable to translational control. Columns 10-12 contain similar rates for propellant consumption that is chargeable to rotational control.

4.2.1 Uncompensated Response Calculations

Linear accelerations appearing in the uncompensated response matrices (Tables 7-9) are calculated by use of the equation

†The compensation mode is internally defaulted to ROT if the user specifies FULL compensation for the vernier jets.

††In Tables 7-14, each matrix is partitioned into two 12 x 6 arrays, simply for the purpose of fitting it conveniently on a page. Command identification mnemonics are tabulated in a column to the left of each matrix partition.

Table 7. Uncompensated Response Matrix for Jet Select Option V

CMD	LINEAR ACCELERATION (FT/SEC^2)			ANGULAR ACCELERATION (RAD/SEC^2)		
	a_x	a_y	a_z	α_x	α_y	α_z
+X	0.00000	0.00000	0.00000	0.00000	0.00000	0.00000
-X	0.00000	0.00000	0.00000	0.00000	0.00000	0.00000
+Y	0.00000	0.00000	0.00000	0.00000	0.00000	0.00000
-Y	0.00000	0.00000	0.00000	0.00000	0.00000	0.00000
+Z	0.00000	0.00000	0.00000	0.00000	0.00000	0.00000
-Z	0.00000	0.00000	0.00000	0.00000	0.00000	0.00000
+ROL	0.00000	0.00000	-0.00386	0.00027	-0.00015	0.00001
-ROL	0.00000	0.00000	-0.00386	-0.00027	-0.00015	-0.00001
+PCH	-0.00026	0.00000	-0.00566	0.00000	0.00035	0.00000
-PCH	0.00000	0.00000	-0.00772	-0.00000	-0.00029	0.00000
+YAW	0.00000	-0.00386	-0.00010	-0.00015	-0.00000	0.00013
-YAW	0.00000	0.00386	-0.00010	0.00015	-0.00000	-0.00013

CMD	PROPELLANT CONSUMPTION RATES (LB/SEC)					
	TRANSLATIONAL CONTROL			ROTATIONAL CONTROL		
	FWD TANK	AFT LEFT TANK	AFT RIGHT TANK	FWD TANK	AFT LEFT TANK	AFT RIGHT TANK
+X	0.00000	0.00000	0.00000	0.00000	0.00000	0.00000
-X	0.00000	0.00000	0.00000	0.00000	0.00000	0.00000
+Y	0.00000	0.00000	0.00000	0.00000	0.00000	0.00000
-Y	0.00000	0.00000	0.00000	0.00000	0.00000	0.00000
+Z	0.00000	0.00000	0.00000	0.00000	0.00000	0.00000
-Z	0.00000	0.00000	0.00000	0.00000	0.00000	0.00000
+ROL	0.00000	0.00000	0.00000	0.00000	0.09230	0.00000
-ROL	0.00000	0.00000	0.00000	0.00000	0.00000	0.09230
+PCH	0.00000	0.00000	0.00000	0.18460	0.00000	0.00000
-PCH	0.00000	0.00000	0.00000	0.00000	0.09230	0.09230
+YAW	0.00000	0.00000	0.00000	0.00000	0.00000	0.09230
-YAW	0.00000	0.00000	0.00000	0.00000	0.09230	0.00000

(See Table 15 for Orbiter Mass Properties)

Table 8. Uncompensated Response Matrix for Jet Select Option P

CMD	LINEAR ACCELERATION (FT/SEC^2)			ANGULAR ACCELERATION (RAD/SEC^2)		
	a_x	a_y	a_z	α_x	α_y	α_z
+X	0.27564	0.00000	0.04861	-0.00001	-0.00033	0.00001
-X	-0.28291	0.00000	0.03857	-0.00002	-0.00211	-0.00001
+Y	-0.00423	0.28055	0.00158	0.00707	-0.00030	0.00365
-Y	-0.00423	-0.28055	0.00158	-0.00708	-0.00031	-0.00365
+Z	0.00420	0.00000	0.42040	-0.00007	0.00109	-0.00000
-Z	0.19200	0.00000	-0.55685	0.00010	0.00061	0.00001
+ROL	0.05492	0.04420	0.05217	0.01591	0.00184	-0.00050
-ROL	0.05492	-0.04420	0.05217	-0.01590	0.00181	0.00050
+PCH	0.00032	0.00000	0.07415	0.00013	0.02225	0.00000
-PCH	0.09537	0.00000	-0.03505	-0.00008	-0.01437	0.00000
+YAW	-0.00423	0.00050	0.00158	-0.00345	-0.00031	0.01238
-YAW	-0.00423	-0.00050	0.00158	0.00345	-0.00030	-0.01238

CMD	PROPELLANT CONSUMPTION RATES (LB/SEC)					
	TRANSLATIONAL CONTROL			ROTATIONAL CONTROL		
	FWD TANK	AFT LEFT TANK	AFT RIGHT TANK	FWD TANK	AFT LEFT TANK	AFT RIGHT TANK
+X	0.00000	3.10710	3.10710	0.00000	0.00000	0.00000
-X	6.21420	0.00000	0.00000	0.00000	0.00000	0.00000
+Y	3.10710	3.10710	0.00000	0.00000	0.00000	0.00000
-Y	3.10710	0.00000	3.10710	0.00000	0.00000	0.00000
+Z	3.10710	3.10710	3.10710	0.00000	0.00000	0.00000
-Z	6.21420	6.21420	6.21420	0.00000	0.00000	0.00000
+ROL	0.00000	0.00000	0.00000	0.00000	3.10710	3.10710
-ROL	0.00000	0.00000	0.00000	0.00000	3.10710	3.10710
+PCH	0.00000	0.00000	0.00000	6.21420	3.10710	3.10710
-PCH	0.00000	0.00000	0.00000	3.10710	3.10710	3.10710
+YAW	0.00000	0.00000	0.00000	3.10710	0.00000	3.10710
-YAW	0.00000	0.00000	0.00000	3.10710	3.10710	0.00000

(See Table 15 for Orbiter Mass Properties)

Table 9. Uncompensated Response Matrix for Jet Select Option PZI

CMD	LINEAR ACCELERATION (FT/SEC^2)			ANGULAR ACCELERATION (RAD/SEC^2)		
	a_x	a_y	a_z	α_x	α_y	α_z
+X	0.27564	0.00000	0.04861	-0.00001	-0.00033	0.00001
-X	-0.28291	0.00000	0.03857	-0.00002	-0.00211	-0.00001
+Y	-0.00423	0.28055	0.00158	0.00707	-0.00030	0.00365
-Y	-0.00423	-0.28055	0.00158	-0.00708	-0.00031	-0.00365
+Z	-0.00727	0.00000	0.08718	-0.00003	-0.00244	-0.00000
-Z	0.19200	0.00000	-0.55685	0.00010	0.00061	0.00001
+ROL	0.05025	0.05578	-0.08776	0.00687	-0.00294	-0.00123
-ROL	0.05025	-0.05578	-0.08778	-0.00688	-0.00296	0.00123
+PCH	-0.00901	0.00000	-0.20574	0.00012	0.01269	0.00000
-PCH	0.10050	0.00000	-0.17556	-0.00001	-0.00590	0.00000
+YAW	-0.00423	0.00050	0.00158	-0.00345	-0.00031	0.01238
-YAW	-0.00423	-0.00050	0.00158	0.00345	-0.00030	-0.01238

CMD	PROPELLANT CONSUMPTION RATES (LB/SEC)					
	TRANSLATIONAL CONTROL			ROTATIONAL CONTROL		
	FWD TANK	AFT LEFT TANK	AFT RIGHT TANK	FWD TANK	AFT LEFT TANK	AFT RIGHT TANK
+X	0.00000	3.10710	3.10710	0.00000	0.00000	0.00000
-X	6.21420	0.00000	0.00000	0.00000	0.00000	0.00000
+Y	3.10710	3.10710	0.00000	0.00000	0.00000	0.00000
-Y	3.10710	0.00000	3.10710	0.00000	0.00000	0.00000
+Z	6.21420	3.10710	3.10710	0.00000	0.00000	0.00000
-Z	6.21420	6.21420	6.21420	0.00000	0.00000	0.00000
+ROL	0.00000	0.00000	0.00000	0.00000	3.10710	0.00000
-ROL	0.00000	0.00000	0.00000	0.00000	0.00000	3.10710
+PCH	0.00000	0.00000	0.00000	6.21420	0.00000	0.00000
-PCH	0.00000	0.00000	0.00000	0.00000	3.10710	3.10710
+YAW	0.00000	0.00000	0.00000	3.10710	0.00000	3.10710
-YAW	0.00000	0.00000	0.00000	3.10710	3.10710	0.00000

(See Table 15 for Orbiter Mass Properties)

Table 10. Rotationally Compensated Response Matrix for Jet Select Option V

CMD	LINEAR ACCELERATION (FT/SEC^2)			ANGULAR ACCELERATION (RAD/SEC^2)		
	a_x	a_y	a_z	α_x	α_y	α_z
+X	0.00000	0.00000	0.00000	0.00000	0.00000	0.00000
-X	0.00000	0.00000	0.00000	0.00000	0.00000	0.00000
+Y	0.00000	0.00000	0.00000	0.00000	0.00000	0.00000
-Y	0.00000	0.00000	0.00000	0.00000	0.00000	0.00000
+Z	0.00000	0.00000	0.00000	0.00000	0.00000	0.00000
-Z	0.00000	0.00000	0.00000	0.00000	0.00000	0.00000
+ROL	-0.00011	0.00029	-0.00622	0.00028	0.00000	0.00000
-ROL	-0.00011	-0.00028	-0.00623	-0.00028	0.00000	0.00000
+PCH	-0.00026	-0.00000	-0.00571	-0.00000	0.00035	0.00000
-PCH	0.00000	0.00000	-0.00773	0.00000	-0.00029	0.00000
+YAW	-0.00006	-0.00386	-0.00372	-0.00000	0.00000	0.00014
-YAW	-0.00006	0.00386	-0.00375	0.00000	0.00000	-0.00014

CMD	PROPELLANT CONSUMPTION RATES (LB/SEC)					
	TRANSLATIONAL CONTROL			ROTATIONAL CONTROL		
	FWD TANK	AFT LEFT TANK	AFT RIGHT TANK	FWD TANK	AFT LEFT TANK	AFT RIGHT TANK
+X	0.00000	0.00000	0.00000	0.00000	0.00000	0.00000
-X	0.00000	0.00000	0.00000	0.00000	0.00000	0.00000
+Y	0.00000	0.00000	0.00000	0.00000	0.00000	0.00000
-Y	0.00000	0.00000	0.00000	0.00000	0.00000	0.00000
+Z	0.00000	0.00000	0.00000	0.00000	0.00000	0.00000
-Z	0.00000	0.00000	0.00000	0.00000	0.00000	0.00000
+ROL	0.00000	0.00000	0.00000	0.07682	0.09914	0.00000
-ROL	0.00000	0.00000	0.00000	0.07708	0.00000	0.09908
+PCH	0.00000	0.00000	0.00000	0.18460	-0.00004	0.00109
-PCH	0.00000	0.00000	0.00000	0.00000	0.09249	0.09230
+YAW	0.00000	0.00000	0.00000	0.04600	0.05296	0.09230
-YAW	0.00000	0.00000	0.00000	0.04635	0.09230	0.05341

(See Table 15 for Orbiter Mass Properties)

Table 11. Rotationally Compensated Response Matrix for Jet Select Option P

CMD	LINEAR ACCELERATION (FT/SEC^2)			ANGULAR ACCELERATION (RAD/SEC^2)		
	a_x	a_y	a_z	α_x	α_y	α_z
+X	0.27570	0.00001	0.04973	0.00000	0.00000	0.00000
-X	-0.28274	0.00003	0.04572	-0.00000	-0.00000	0.00000
+Y	0.02797	0.25772	0.02775	0.00000	0.00000	0.00000
-Y	0.02811	-0.25769	0.02780	-0.00000	0.00000	0.00000
+Z	0.01172	0.00021	0.41798	0.00000	-0.00000	0.00000
-Z	0.19652	-0.00029	-0.55801	0.00000	-0.00000	0.00000
+ROL	0.06689	0.04422	0.04777	0.01576	0.00000	-0.00000
-ROL	0.06670	-0.04422	0.04783	-0.01578	-0.00000	0.00000
+PCH	0.00077	-0.00036	0.07458	0.00000	0.02226	-0.00000
-PCH	0.09567	0.00024	-0.03477	0.00000	-0.01436	-0.00000
+YAW	0.00768	0.01009	0.01258	-0.00000	-0.00000	0.01227
-YAW	0.00767	-0.01008	0.01256	0.00000	0.00000	-0.01227

CMD	PROPELLANT CONSUMPTION RATES (LB/SEC)					
	TRANSLATIONAL CONTROL			ROTATIONAL CONTROL		
	FWD TANK	AFT LEFT TANK	AFT RIGHT TANK	FWD TANK	AFT LEFT TANK	AFT RIGHT TANK
+X	0.00000	3.10710	3.10710	0.09260	0.04962	0.04812
-X	6.21420	0.00000	0.00000	0.59174	0.30238	0.30422
+Y	3.10710	3.10710	0.00000	1.22951	2.78601	1.80583
-Y	3.10710	0.00000	3.10710	1.23580	1.81306	2.79308
+Z	3.10710	3.10710	3.10710	0.23769	0.25121	0.25242
-Z	6.21420	6.21420	6.21420	0.13789	0.15948	0.15659
+ROL	0.00000	0.00000	0.00000	0.52082	3.50274	3.62792
-ROL	0.00000	0.00000	0.00000	0.51543	3.62253	3.49672
+PCH	0.00000	0.00000	0.00000	6.21561	3.13390	3.13249
-PCH	0.00000	0.00000	0.00000	3.10673	3.12332	3.12369
+YAW	0.00000	0.00000	0.00000	3.08110	0.66113	3.76823
-YAW	0.00000	0.00000	0.00000	3.08020	3.76692	0.65982

(See Table 15 for Orbiter Mass Properties)

Table 12. Rotationally Compensated Response Matrix for Jet Select Option PZI

CMD	LINEAR ACCELERATION (FT/SEC^2)			ANGULAR ACCELERATION (RAD/SEC^2)		
	a_x	a_y	a_z	α_x	α_y	α_z
+X	0.27551	0.00003	0.04306	-0.00000	-0.00000	-0.00000
-X	-0.28410	0.00004	0.00346	-0.00000	-0.00000	0.00000
+Y	0.05361	0.21093	-0.17340	0.00000	0.00000	0.00000
-Y	0.05320	-0.21147	-0.17220	-0.00000	-0.00000	0.00000
+Z	-0.00861	0.00007	0.04659	-0.00000	0.00000	0.00000
-Z	0.20320	-0.00091	-0.57729	0.00000	-0.00000	0.00000
+ROL	0.04772	0.05583	-0.13582	0.00855	-0.00000	0.00000
-ROL	0.04771	-0.05583	-0.13601	-0.00851	-0.00000	0.00000
+PCH	-0.00811	-0.00101	-0.20731	0.00000	0.01264	0.00000
-PCH	0.10054	0.00004	-0.17563	0.00000	-0.00590	0.00000
+YAW	0.01963	0.02839	-0.07113	-0.00000	0.00000	0.01176
-YAW	0.01981	-0.02880	-0.07157	0.00000	0.00000	-0.01175

CMD	PROPELLANT CONSUMPTION RATES (LB/SEC)					
	TRANSLATIONAL CONTROL			ROTATIONAL CONTROL		
	FWD TANK	AFT LEFT TANK	AFT RIGHT TANK	FWD TANK	AFT LEFT TANK	AFT RIGHT TANK
+X	0.00000	3.10710	3.10710	0.16445	0.00593	0.00267
-X	6.21420	0.00000	0.00000	1.04597	0.01244	0.01226
+Y	3.10710	3.10710	0.00000	3.30729	1.30124	3.86593
-Y	3.10710	0.00000	3.10710	3.29051	3.33737	1.29356
+Z	6.21420	3.10710	3.10710	1.20723	0.01599	0.01250
-Z	6.21420	6.21420	6.21420	0.03107	0.32969	0.37291
+ROL	0.00000	0.00000	0.00000	1.78465	3.10710	0.30338
-ROL	0.00000	0.00000	0.00000	1.77134	0.33933	3.10710
+PCH	0.00000	0.00000	0.00000	6.22035	0.00815	0.05599
-PCH	0.00000	0.00000	0.00000	0.00051	3.10997	3.10710
+YAW	0.00000	0.00000	0.00000	3.97754	1.55344	3.10710
-YAW	0.00000	0.00000	0.00000	3.98115	3.10710	1.56497

(See Table 15 for Orbiter Mass Properties)

Table 13. Fully Compensated Response Matrix for Jet Select Option P

CMD	LINEAR ACCELERATION (FT/SEC^2)			ANGULAR ACCELERATION (RAD/SEC^2)		
	a_x	a_y	a_z	α_x	α_y	α_z
+X	0.29321	0.00000	0.00000	0.00000	-0.00000	0.00000
-X	-0.28664	-0.00000	-0.00000	0.00000	-0.00000	0.00000
+Y	0.00000	0.25770	-0.00000	0.00000	0.00000	0.00000
-Y	0.00000	-0.25770	-0.00000	-0.00000	0.00000	0.00000
+Z	0.00000	0.00000	0.41990	0.00000	0.00000	0.00000
-Z	-0.00000	0.00000	-0.52620	0.00000	-0.00000	0.00000
+ROL	-0.00000	0.00000	-0.00000	0.01576	0.00000	-0.00000
-ROL	-0.00000	-0.00000	-0.00000	-0.01578	-0.00000	0.00000
+PCH	-0.00000	0.00000	-0.00000	0.00000	0.02226	-0.00000
-PCH	0.00000	0.00000	-0.00000	0.00000	-0.01436	-0.00000
+YAW	0.00000	0.00000	0.00000	-0.00000	0.00000	0.01227
-YAW	-0.00000	0.00000	0.00000	0.00000	0.00000	-0.01227

CMD	PROPELLANT CONSUMPTION RATES (LB/SEC)					
	TRANSLATIONAL CONTROL			ROTATIONAL CONTROL		
	FWD TANK	AFT LEFT TANK	AFT RIGHT TANK	FWD TANK	AFT LEFT TANK	AFT RIGHT TANK
+X	0.55370	3.66093	3.66080	0.10483	0.06375	0.06195
-X	6.72346	0.50914	0.50926	0.60309	0.31552	0.31716
+Y	4.36788	3.48822	0.38112	1.32173	2.83860	1.85349
-Y	4.37231	0.38197	3.48907	1.32839	1.86584	2.84595
+Z	3.36767	3.10710	3.10964	0.26327	0.26524	0.26733
-Z	10.53718	6.21738	6.21420	0.55050	0.37253	0.36992
+ROL	3.39348	0.75765	1.29059	0.95004	3.93589	4.22944
-ROL	3.38941	1.29116	0.75770	0.94316	4.22245	3.92862
+PCH	1.51900	0.88758	0.88278	6.29723	3.19159	3.18844
-PCH	2.69513	0.44032	0.44342	3.34612	3.26020	3.26223
+YAW	0.61690	0.17831	0.29988	3.16365	0.75217	3.89763
-YAW	0.61564	0.29943	0.17787	3.16236	3.39589	0.75045

(See Table 15 for Orbiter Mass Properties)

Table 14. Fully Compensated Response Matrix for Jet Select Option PZI

CMD	LINEAR ACCELERATION (FT/SEC^2)			ANGULAR ACCELERATION (RAD/SEC^2)		
	a_x	a_y	a_z	α_x	α_y	α_z
+X	0.29067	-0.00000	0.00000	-0.00000	-0.00000	0.00000
-X	-0.28288	0.00000	0.00000	-0.00000	-0.00000	0.00000
+Y	0.00000	0.21120	-0.00000	0.00000	0.00000	0.00000
-Y	-0.00000	-0.21120	-0.00000	-0.00000	-0.00000	0.00000
+Z	-0.00000	-0.00000	0.04787	-0.00000	-0.00000	-0.00000
-Z	0.00000	-0.00000	-0.57553	0.00000	-0.00000	0.00000
+ROL	-0.00000	-0.00000	0.00000	0.00655	-0.00000	-0.00000
-ROL	0.00000	-0.00000	0.00000	-0.00651	-0.00000	0.00000
+PCH	-0.00000	-0.00000	0.00000	-0.00000	0.01264	0.00000
-PCH	-0.00000	-0.00000	0.00000	-0.00000	-0.00590	0.00000
+YAW	-0.00000	-0.00000	-0.00000	-0.00000	-0.00000	0.01176
-YAW	-0.00000	-0.00000	0.00000	0.00000	0.00000	-0.01175

CMD	PROPELLANT CONSUMPTION RATES (LB/SEC)					
	TRANSLATIONAL CONTROL			ROTATIONAL CONTROL		
	FWD TANK	AFT LEFT TANK	AFT RIGHT TANK	FWD TANK	AFT LEFT TANK	AFT RIGHT TANK
+X	0.46330	3.57088	3.57040	0.16626	0.02999	0.03030
-X	6.25160	0.03693	0.03740	1.04765	0.01498	0.01467
+Y	26.67336	14.65366	11.54656	7.87348	1.36162	3.91333
-Y	26.50964	11.46686	14.57396	7.82500	3.89733	1.34563
+Z	6.21528	3.20395	3.20503	1.21355	0.01751	0.01304
-Z	10.67678	6.22715	6.21420	0.79452	0.34402	0.39780
+ROL	25.69667	12.12785	12.95239	7.45309	4.18962	0.70408
-ROL	25.76410	12.98288	12.16461	7.47731	0.72213	4.18116
+PCH	27.05628	14.04470	14.03455	11.51797	0.08930	0.13194
-PCH	25.02923	11.76977	11.77451	4.82657	3.18031	3.16041
+YAW	13.23199	6.30440	6.72368	6.90517	2.10436	3.30836
-YAW	13.34197	6.77696	6.35791	6.93498	3.31869	2.11534

(See Table 15 for Orbiter Mass Properties)

Table 15. Typical Orbiter Mass Properties

ITEM	DESCRIPTION	VALUE
1	WEIGHT....................................	200017.0000 LB
2	IXX.......................................	887302.0000 SLUG-FT^2
3	IYY.......................................	6366877.0000 SLUG-FT^2
4	IZZ.......................................	6694367.0000 SLUG-FT^2
5	IYZ.......................................	-971.0000 SLUG-FT^2
6	IZX.......................................	247376.0000 SLUG-FT^2
7	IXY.......................................	5622.0000 SLUG-FT^2
8	CG STA....................................	1095.3000 IN
9	CG BL.....................................	0.3000 IN
10	CG WL.....................................	377.4000 IN
11	SENSOR STA................................	500.7000 IN
12	SENSOR BL.................................	132.0000 IN
13	SENSOR WL.................................	446.1000 IN
14	SENSOR AXES PITCH.........................	90.0000 DEG
15	SENSOR AXES YAW...........................	0.0000 DEG
16	SENSOR AXES ROLL..........................	-67.0000 DEG
17	DAP CYCLE.................................	80.0000 MILLISEC

$$\bar{a} = (32.174/W) \begin{bmatrix} \Sigma F_{xj} \\ \Sigma F_{yj} \\ \Sigma F_{zj} \end{bmatrix} \quad , \tag{4}$$

where W is the Orbiter gross weight and where ΣF_{xj}, ΣF_{yj}, and ΣF_{zj} represent the sums of thrust components (from Table 1) for all of the thrusters that are designated in the appropriate jet select table (Tables 4-6) to be fired for the purpose of implementing the command under consideration. The corresponding angular accelerations are given by

$$\bar{\alpha} = \bar{\bar{q}} \circ \bar{\alpha}' \circ \tilde{\tilde{q}} \quad , \tag{5}$$

where

$$\bar{\alpha}' = \begin{bmatrix} L_x'/I_{xx}' \\ L_y'/I_{yy}' \\ L_z'/I_{zz}' \end{bmatrix} \quad , \tag{6}$$

$$\bar{L}' \equiv \begin{bmatrix} L_x' \\ L_y' \\ L_z' \end{bmatrix} = \tilde{\tilde{q}} \circ \Sigma \bar{L}_j \circ \bar{\bar{q}} \quad , \tag{7}$$

and where $\Sigma \bar{L}_j$ represents the sum of the individual torque vectors produced by the designated thrusters, as calculated from Equations (1) through (3). The symbols I_{xx}', I_{yy}', and I_{zz}' represent the Orbiter's principal moments of inertia, and primed vectors represent those whose components are measured along the corresponding principal axes.

Expressions (5) and (7) are coordinate transformation equations (see Reference 1) in which $\bar{\bar{q}}$ represents the unit quaternion that defines the angular displacement of the Orbiter's principal axes of inertia with respect to to body axes, and $\tilde{\tilde{q}}$ represents its conjugate. The quaternion $\bar{\bar{q}}$ is computed internally by the HFRMP in such a manner that the associated rotation of coordinates will transform the inertia tensor

$$[I] = \begin{bmatrix} I_{xx} & -I_{xy} & -I_{zx} \\ -I_{xy} & I_{yy} & -I_{yz} \\ -I_{zx} & -I_{yz} & I_{zz} \end{bmatrix} \qquad (8)$$

(which is composed of user-specified moments and products of inertia about the Orbiter's body axes) into the diagonal form

$$[I'] = \begin{bmatrix} I'_{xx} & 0 & 0 \\ 0 & I'_{yy} & 0 \\ 0 & 0 & I'_{zz} \end{bmatrix} . \qquad (9)$$

Propellant flow rates (columns 7-12) are assumed to be 3.1071 lb/sec for each active primary jet and 0.0923 lb/sec for each active vernier jet. These rates are based on the nominal vacuum thrust magnitudes (870 lb and 24 lb) and specific impulses (280 sec and 260 sec) that are given in Reference 7. Each thruster is assumed always to be fed from its nominal source (tank), no provisions are made for simulating propellant cross-feed.

4.2.2 Compensated Response Calculations

The compensated response matrices (Tables 10-14) are obtained by performing elementary row operations on the uncompensated response matrices (Tables 7-9). Specifically, appropriate rows in the uncompensated matrix are multiplied by positive factors and added to other rows in such a manner as to null the unwanted cross-coupling accelerations. The positive factors represent idealized ratios (calculated without regard to minimum-impulse or other limitations) of the firing time required of the compensating jets with respect to the firing time of the jets activated by the primary command.

The results of the computations described in the preceding paragraph are such that propellant consumed in the process of nulling cross-coupled angular accelerations is charged to rotational control, and that which is consumed in the process of nulling cross-coupled linear accelerations is charged to translational control, regardless of the nature of the primary command.

4.3 ATTITUDE CONTROL LOGIC

For the purpose of (1) applying an angular velocity impulse at the beginning of a flight profile segment or (2) exercising rate-hold control (IRH or LVRH) within a segment, the HFRMP always applies rotational cross-coupling compensation, whether or not such compensation has been specified by the user.[†] For the aforementioned purposes, the compensation mode is internally defaulted to ROT if the user has specified NONE; otherwise, the user's specification is applied.

4.3.1 Angular Velocity Impulses

At the beginning of each flight profile segment, the HFRMP determines the direction and magnitude of the instantaneous angular rate increment that is to be applied about each of the Orbiter's body axes. These three increments may be supplied directly by the user (the most common specification being zero for all three components), or they may be calculated internally to yield user-specified final (post-impulse) rates with respect to inertial space or the Orbiter's local vertical frame. For each axis, an effective thruster firing time is then calculated by dividing an angular acceleration into the angular velocity increment, the acceleration being obtained from the appropriate row (+ROL, -ROL, +PCH, -PCH, +YAW, or -YAW) and column (4, 5, or 6) of the applicable response matrix (Table 10, 11, 12, 13, or 14). The entire row of the matrix is then multiplied by the effective firing time, and the resulting linear velocity, angular velocity, and propellant consumption increments are added immediately to the appropriate state variables and propellant accounts.

4.3.2 Rate-Hold Control

The HFRMP trajectory integration step size typically is several orders of magnitude greater than the DAP cycle time; therefore, it is not practicable to simulate the individual thruster firing pulses that are commanded by the

---

[†]The reasoning here is that it makes little difference in the long run whether the effects of rotational cross-coupling are removed immediately upon implementation of a primary command, or a short time later when the pilot or the DAP determines (on the basis of angular velocity and/or displacement errors detected by the IMU) that a corrective command is required.

real-world DAP for the purpose of maintaining the Orbiter attitude within specified deadbands. The long-term effects of pulsed thruster firings are simulated in the HFRMP by integrating the average accelerations and propellant consumption rates that result from such pulses. An idealized and very greatly simplified control logic is used for this purpose. The rationale is that if the idealized logic is designed to minimize the average propellant consumption, subject to the basic constraints of the real system, it will produce essentially the same long-term effects as the real-world DAP.

At a given instant of time, suppose that inertial effects and natural torque (due to aerodynamics and the gravity gradient) are such that, if not counteracted by the attitude control jets, they would produce an undesired angular acceleration component of magnitude ν about one of the Orbiter's body axes. When the user specifies the IRH option, ν represents the appropriate body-axis component of the Orbiter's total natural acceleration (relative to inertial space); when LVRH is specified, it represents the difference between the natural acceleration of the Orbiter and that of its local-vertical reference frame.

For the purpose of calculating average effects of the control system response, we treat ν as if it were a constant, and write the equations

$$\omega = \omega_0 + \nu t \tag{10}$$

and

$$\theta = \theta_0 + \omega_0 t + \tfrac{1}{2}\nu t^2 \quad , \tag{11}$$

to describe the uncontrolled angular velocity and angular displacement (about the axis under consideration) as functions of time.

The purpose of the attitude control logic is to maintain the angular displacement θ within the limits of -D and +D, where D represents the user-specified deadband width, in such a manner as to minimize the RCS propellant consumption. Figure 1 illustrates an idealized case[†] in which $\theta_0 = D$ and $\omega_0 = -\frac{1}{2}\Delta\omega_{opt}$, where

$$\Delta\omega_{opt} = 4\sqrt{D\nu} \tag{12}$$

represents the magnitude of a uniform corrective rate increment that is applied at a regular interval

$$\tau_{max} = 4\sqrt{D/\nu} \quad . \tag{13}$$

Equations (12) and (13) are obtained by solving Equations (10) and (11) for the angular velocity increment that minimizes the average propellant consumption rate, which (for any value of $-2\omega_0 = \Delta\omega \leq 4\sqrt{D\nu}$) is given by

$$\underline{\dot{W}} = (T/\tau)\ \dot{W}_\alpha \quad , \tag{14}$$

where $\dot{W}_\alpha$ is the steady-state consumption rate of the thrusters which oppose the natural acceleration (i.e., $\dot{W}_\alpha$ is the sum of columns 7-12 from the appropriate row of Table 10, 11, 12, 13, or 14), T is the electrical pulse width of the corrective thruster firing, and

$$\tau = \Delta\omega/\nu \tag{15}$$

is the interval between pulses. The magnitude of the angular velocity increment is related to T by the equation

$$\Delta\omega = \alpha T^* \quad , \tag{16}$$

where

[†]The idealization consists of using angular velocity impulses to represent thruster firings, and of making the magnitude of ω_0 precisely half the magnitude of the corrective impulse $\Delta\omega$. This is the average magnitude of ω_0, which is randomly distributed between 0 and $\Delta\omega$ in the real world.

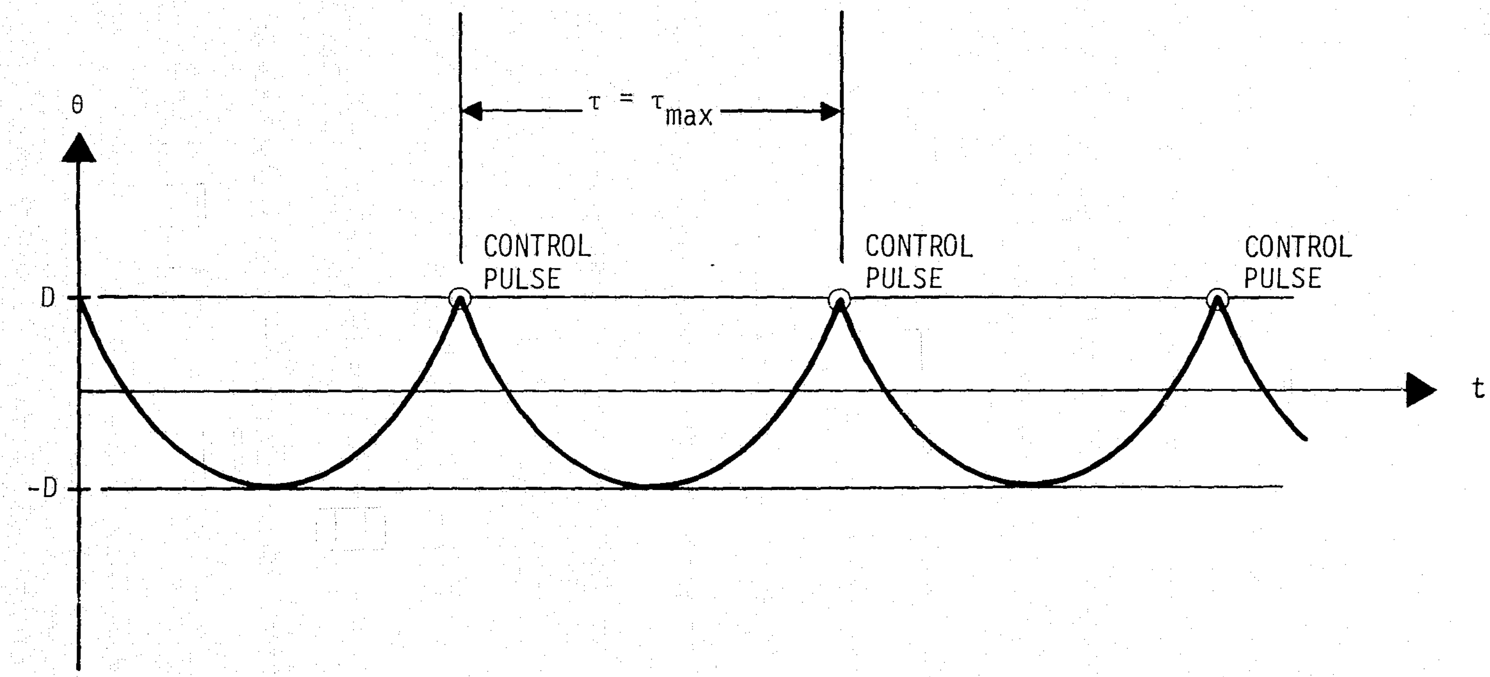

Figure 1. Optimally-Controlled Angular Displacement History

$$T^* = T - .014 \text{ seconds} \tag{17}$$

is the effective pulse width and where α is the magnitude of the steady-state angular acceleration produced by the control jets that oppose the natural acceleration.

When (15), (16), and (17) are substituted into Equation (14), the average propellant consumption rate is found to be related to $\Delta\omega$ by the expression

$$\underline{\dot{W}} = \left(1 + \frac{.014\alpha}{\Delta\omega}\right) \frac{\dot{W}_\alpha \nu}{\alpha} \quad . \tag{18}$$

Equation (18) shows clearly that the average propellant consumption rate increases when the angular displacement is undercontrolled (i.e., when $\Delta\omega < 4\sqrt{D\nu}$), as illustrated in Figure 2. If $-2\omega_0 = \Delta\omega > 4\sqrt{D\nu}$, then it becomes necessary to apply control pulses at both the upper and the lower deadband limits, as illustrated in Figure 3. This represents an overcontrolled situation that is even more inefficient than undercontrol, because it results in the alternate firing of thrusters that oppose each other. Clearly then, in the idealized case under consideration, the optimum value of $\Delta\omega$ is given by Equation (12), from which we obtain

$$T_{opt} = 4\sqrt{D\nu}/\alpha + .014 \text{ seconds} \tag{19}$$

for the optimum electrical pulse width of the average corrective impulse.

So far, we have treated T as if it were a continuous variable. However, in the real world, T must be an integer multiple of the DAP cycle time C. Therefore, we write

$$T = NC \quad , \tag{20}$$

where

$$N = \text{MAX}\,(1, \text{INT}\,(T_{opt}/C)) \quad . \tag{21}$$

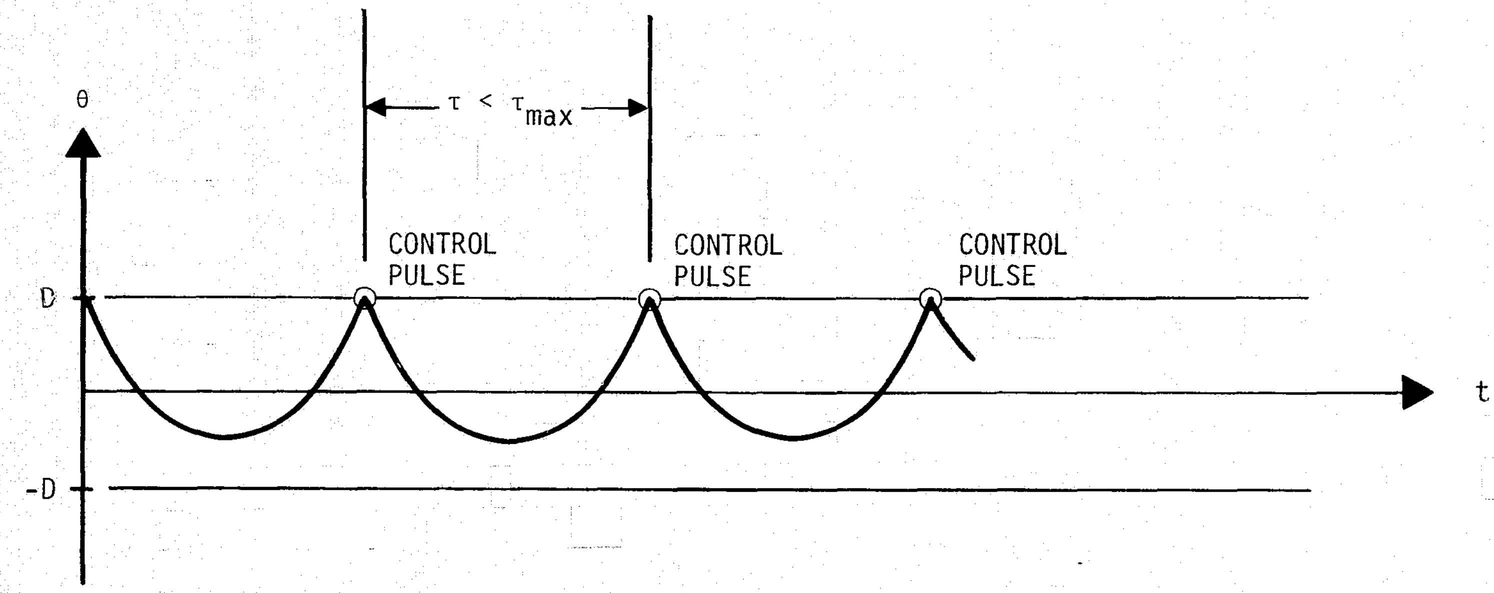

Figure 2. Undercontrolled Angular Displacement History

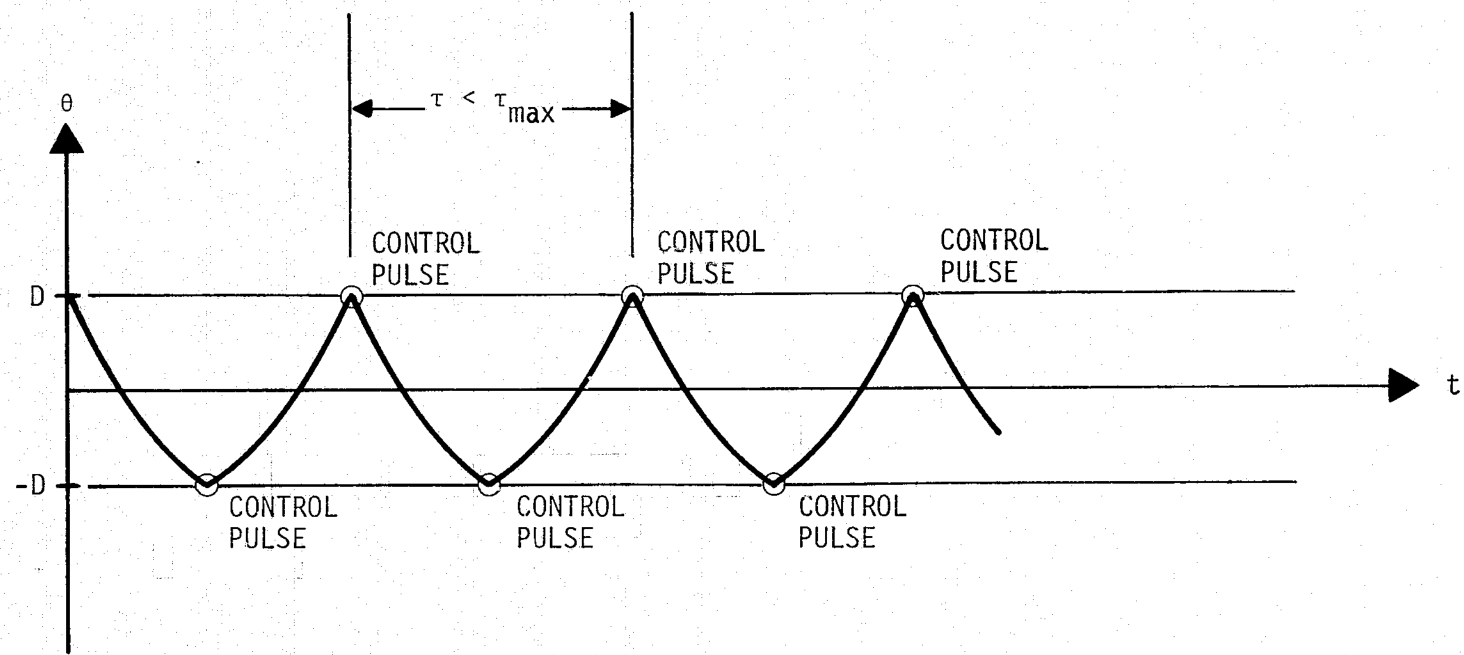

Figure 3. Overcontrolled Angular Displacement History

and where T_{opt} is obtained from Equation (19). The function MAX (X,Y) represents the maximum value of the arguments X and Y, and the function INT (Z) represents the integer part of the argument Z.

Equations (20) and (21) imply that some degree of undercontrol or overcontrol is unavoidably required in the general case. The degree of overcontrol (if any) is reflected in the value of $\underline{\beta}$, which represents the average acceleration magnitude produced by the reinforcing jets (those which produce torque of the same sign as the natural acceleration), and which is given by one or the other of the two equations

$$[\text{If INT } (T_{opt}/C) = 0]: \ \underline{\beta} = (\alpha T^*)^2/16D - \nu \tag{22a}$$

and

$$[\text{If INT } (T_{opt}/C) > 0]: \ \underline{\beta} = 0 \ , \tag{22b}$$

where T^* is given by Equation (17). Equation (22a) can be obtained by substituting αT^* for $\Delta\omega_{opt}$ and $(\nu + \underline{\beta})$ for ν in Equation (12). The value of $\underline{\beta}$ represents the idealized* minimum amount by which the natural acceleration ν must be supplemented in order to balance the counteractive control pulses of fixed magnitude $\alpha T^* = \alpha$ (NC - 0.14).

After having calculated $\underline{\beta}$, the average magnitude of the counteractive jet acceleration is obtained from the equation

$$\underline{\alpha} = \nu + \underline{\beta} \ , \tag{23}$$

which describes the aforementioned balance of average accelerations.

---

*To arrive at Equation (22a), the acceleration from the reinforcing jets is treated as if it acted continuously at the average level. A greater value, approaching $\underline{\beta} = (\alpha T^*)^2/8D - \nu$ as ν approaches zero, would be obtained if $\underline{\beta}$ were treated as the average resulting from uniform angular velocity impulses applied at the lower deadband limit. The use of Equation (22a) is justified on the basis of the better agreement between the results it produces and those produced by more detailed simulations of the actual onboard DAP logic (Section 5).

To calculate the average linear and angular acceleration vector components that result from controlling angular motion about the body axis under consideration, the data in columns 1-6 of the appropriate pair of rows (+ROL and -ROL, +PCH and -PCH, or +YAW and -YAW) in the response matrix (Table 10, 11, 12, 13, or 14) are multiplied by the acceleration factors

$$A_{\alpha} = \underline{\alpha}/\alpha \tag{24}$$

and

$$A_{\beta} = \underline{\beta}/\beta \quad , \tag{25}$$

where β represents the steady-state angular acceleration magnitude produced by the reinforcing jets. The factor A_{β} is applied to the row which represents a commanded rotation of the same sign as the natural acceleration component, and A_{α} is applied to the row which represents a commanded rotation of the opposite sign.

To calculate the corresponding propellant consumption rates, columns 7-12 are multiplied by the factors

$$P_{\alpha} = A_{\alpha} \; (T/T^*) \tag{26}$$

and

$$P_{\beta} = A_{\beta} \; (T/T^*) \quad , \tag{27}$$

where, as indicated by Equation (17), T/T^* represents the ratio of the electrical width to the effective width of the average control pulse. Equations (26) and (27) represent an implicit variation of specific impulse (I_{SP}) with electrical pulse width. This variation is illustrated for the PRCS jets in Figure 4, where the implicitly-defined HFRMP values are superimposed on a curve reproduced from Reference 7.

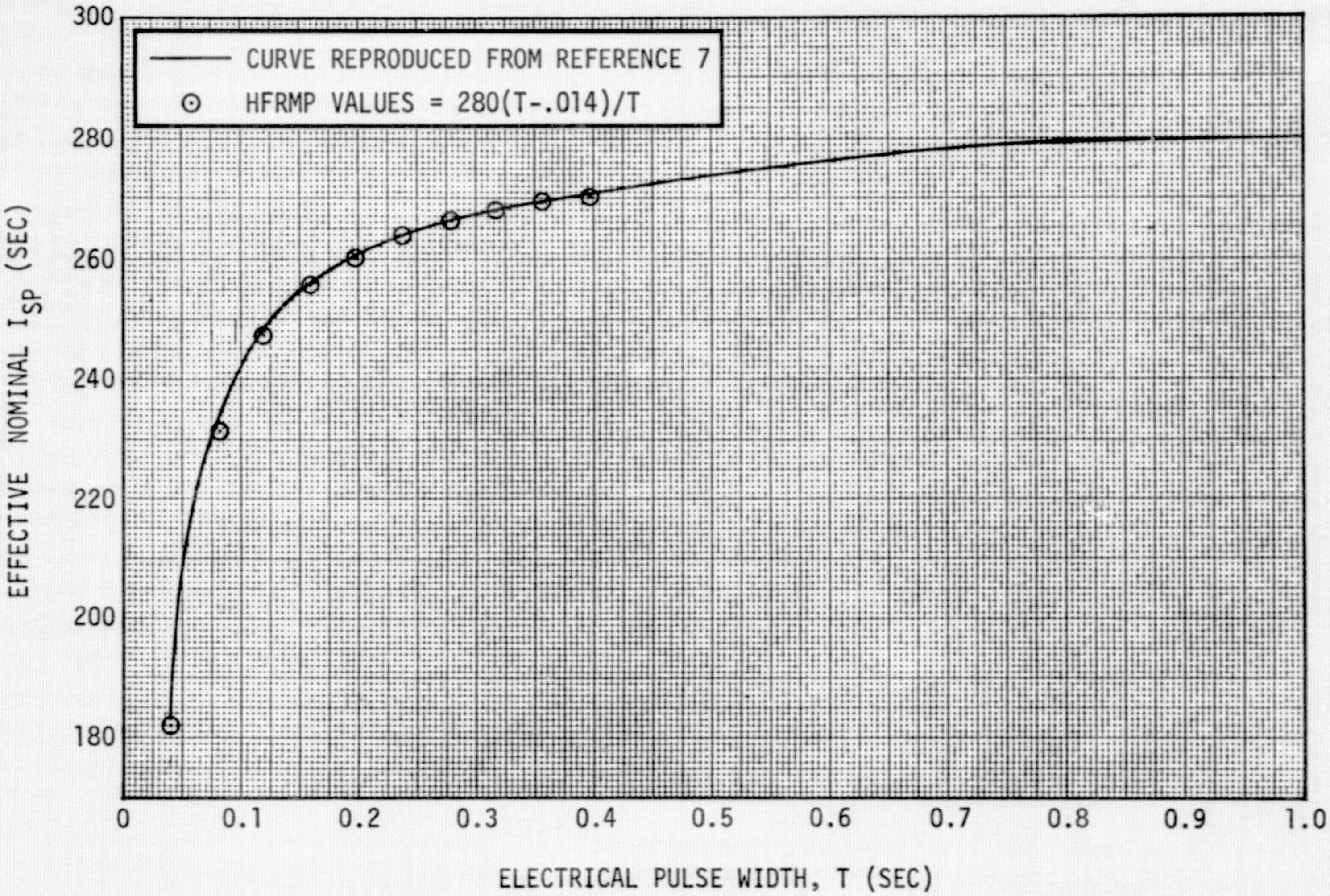

Figure 4. Primary RCS Specific Impulse as a Function of Electrical Pulse Width

The HFRMP performs the calculations defined by Equations (19) through (27), for each one of the Orbiter's three body axes, at every point in the trajectory calculation process where state variable derivatives are computed. The attitude-control propellant consumption rates and the associated components of linear and angular acceleration are summed with their counterparts which are produced by other effects (gravity, aerodynamics, and commanded translational thrust), and then integrated by means of a 4th order Runge-Kutta scheme to calculate the Orbiter's state vector and propellant expenditure as a function of time.

As a final note of interest with respect to the simplified rate-control logic, Equations (19) through (23) indicate that the average acceleration magnitude in each direction of rotation about a given axis is given by

$$\underline{\alpha} = \underline{\beta} = \alpha^2 \quad (C-.014)^2/16D \tag{28}$$

whenever ν is of negligible magnitude. When this result is substituted into Equations (26) and (27), the average propellant consumption rate for attitude control about the axis under consideration is found to be

$$\underline{\dot{W}} = \frac{\alpha C \ (C-.014)}{16D} \ (\dot{W}_\alpha + \frac{\alpha}{\beta} \ \dot{W}_\beta) \quad , \tag{29}$$

where $\dot{W}_\alpha$ and $\dot{W}_\beta$, respectively, are the steady-state propellant consumption rates for the thrusters that oppose and reinforce the natural acceleration. Furthermore, the cited equations indicate that the average consumption rate decreases to a value of

$$\underline{\dot{W}} = \frac{\alpha C \ (C-.014)}{16D} \quad \dot{W}_\alpha \tag{30}$$

when the natural acceleration magnitude increases to the value

$$\nu = [\alpha(C-.014)]^2/16D \quad , \tag{31}$$

and that any further increase in the value of ν causes $\dot{\underline{W}}$ to increase again. Equations (29), (30), and (31) very succinctly illustrate the basic relationships between the DAP cycle time C, the deadband width D, and the average propellant consumption rate due to attitude "deadbanding". The implications of these equations are of course subject to the limitations of the simplified rate-control logic. One of the more significant limitations is the assumption that the natural acceleration is constant everywhere within the attitude deadband. This clearly will not be true when the deadband is very wide.

5. COMPARISON OF HFRMP AND SSFS DATA

For the purpose of verifying the HFRMP OMS/RCS/DAP models, a considerable amount of data were generated with the HFRMP to be compared with similar data which were generated by the Space Shuttle Functional Simulator (SSFS) and published in References 9 and 10. In the SSFS, thruster firing commands are computed at the same frequency as that of the real-world DAP, using a jet-select logic and an idealized limit cycle control law representative of the Shuttle onboard software. As pointed out previously, the HFRMP does not simulate individual RCS thruster firing pulses, but instead calculates the average accelerations and propellant rates that result from such pulses in an attempt to simulate their long-term effects. Aside from this basic difference in simulation technique, the following differences are known to exist between the environmental and Shuttle system models that were used in the two programs:

1. The primary reaction control system (PRCS) thrust and moment data contained in Tables 1-3 differ significantly in some instances from those which were being used in the SSFS when the data were generated for References 9 and 10.

2. Although both programs use the 1962 Standard atmosphere model to calculate density as a function of altitude, altitudes are calculated with respect to a spherical earth in the SSFS. In the HFRMP, altitudes are referenced to the Fischer ellipsoid.

3. The atmosphere is assumed to be stationary (in a geocentric inertial frame) in the SSFS, while in the HFRMP it is assumed to rotate with the earth.

4. The aerodynamic coefficients used in the SSFS (at least during the generation of data for Reference 9) were representative of a doors-closed Orbiter configuration. In the HFRMP, aerodynamic coefficients are calculated from curve-fit equations that include analytical estimates of the effect of open doors.

5.1 PROPELLANT CONSUMPTION

5.1.1 Translational and Rotational Maneuvers

Tables 16 and 17 contain PRCS propellant requirements for different types of translational and rotational maneuvers, as calculated by the SSFS and by the HFRMP. Two different cross coupling compensation options (ROT and FULL) were used in the HFRMP calculations, and the results obtained from both options

Table 16. PRCS Propellant (Lb) Required to Produce a Linear Velocity Increment of One Foot per Second

	COMMANDED DIRECTION OF TRANSLATION				
	+X	-X	±Y	+Z	-Z
SSFS (REF. 9)	27	30	42	23	43
HFRMP (ROT COMP.)	(23)	(26)	(47)	(24)	34
HFRMP (FULL COMP.)	28	34	55	25	(46)

(See Table 15 for Orbiter Mass Properties)

Table 17. PRCS Propellant (lb) Required to Start and Stop a Rotational Maneuver Executed at a Rate of One Degree per Second

	COMMANDED ROTATION		
	ROLL	PITCH	YAW
SSFS (REF. 9)	18	22	24
HFRMP (ROT COMP.)	(17)	(21)	(21)
HFRMP (FULL COMP.)	32	29	25

(See Table 15 for Orbiter Mass Properties)

are contained in the cited tables. For each maneuver type, the circled HFRMP value represents that generated with the compensation option which most nearly approximates the type of compensation applied in the SSFS simulations.

The SSFS data are taken from Reference 9. The attitude deadbands were set at 0.5 degrees per axis and the translational cross coupling thresholds (which must be exceeded before any compensation is applied) were set at 0.3 feet per second per axis for the SSFS calculations. The propellant consumption data were based on simulated linear velocity increments of one foot per second, and angular velocity increments of one degree per second. For maneuvers of this magnitude, the translational cross coupling threshold was exceeded only in the case of -Z translation. Therefore, the HFRMP compensation mode that most closely approximates the SSFS simulation is FULL in the case of -Z translation, while in all other cases it is ROT. No threshold values are involved in the HFRMP compensation logic; the effects of cross-coupled accelerations are either removed completely and instantaneously, or not at all.

Considering the differences in simulation methods and in the basic PRCS force and moment data, the HFRMP propellant consumption values shown in Tables 16 and 17 are reasonably close to those generated by the SSFS. OMS propellant consumption data generated by the two programs were identical: 19.9 pounds for a velocity increment of one foot per second, with an Orbiter gross weight of 200 017 pounds.

5.1.2 VRCS Attitude Maintenance

Table 18 contains vernier reaction control system (VRCS) propellant consumption rates for five different attitude-hold options and six orbit altitudes. These data, taken from Reference 9, were generated by the SSFS with a 40 millisecond DAP cycle time and attitude deadbands of 0.1 degrees per axis. Table 19 contains comparable data which were generated by the HFRMP, using the ROT compensation option and the rate-hold control logic described in Section 4.3.2. The orbit inclination was set at 28.5 degrees for all HFRMP attitude-maintenance runs.

Table 18. SSFS Propellant Consumption Rates (Lb/Hr)† For VRCS Attitude Maintenance, With 40 mSec DAP Cycle

(Deadband = 0.1 Deg/Axis)

	ORBIT ALTITUDE (NAUTICAL MILES)					
ATTITUDE	90	100	120	150	200	500
X POP INERTIAL HOLD	9	6	3	2	1	1
Y POP INERTIAL HOLD	3	3	3	3	2	2
Z POP INERTIAL HOLD	15	10	6	4	4	4
X POP ZLV (HEADS DOWN)	23	13	6	2	1	1
Y POP ZLV (HEADS DOWN)	1	1	1	1	1	1

(See Table 15 for Orbiter Mass Properties)

† - Averaged over a one-orbit period

Table 19. HFRMP Propellant Consumption Rates (Lb/Hr)† For VRCS Attitude Maintenance, With 40 mSec DAP Cycle

(Deadband = 0.1 Deg/Axis)

		ORBIT ALTITUDE (NAUTICAL MILES)					
		90	100	120	150	200	500
ATTITUDE	X POP INERTIAL HOLD	14	7	3	2	2	1
	Y POP INERTIAL HOLD	3	3	3	3	2	2
	Z POP INERTIAL HOLD	17	11	8	6	6	4
	X POP ZLV (HEADS DOWN)	31	17	6	2	1	.4
	Y POP ZLV (HEADS DOWN)	.7	.5	.4	.4	.4	.3

(See Table 15 for Orbiter Mass Properties)

† - Averaged over a one-orbit period

The agreement between the VRCS propellant consumption data produced by the two programs is considered to be excellent except at the two lowest altitudes, where the differences in the atmosphere and aerodynamic models are sufficient to produce significant differences in propellant requirements for the X POP ZLV (Orbiter X axis Perpendicular to the Orbit Plane, Z axis continuously aligned with Local Vertical), the Z POP Inertial Hold, and the X POP Inertial Hold modes.

The data contained in Tables 18 and 19 represent hourly rates, averaged over one orbit period. The presentation of the data in this manner should not be taken to mean that propellant consumption is a linear function of time in all cases. The HFRMP data shown in Figure 5 illustrates that the instantaneous rate can vary significantly over the time span of an orbit period.

5.1.3 PRCS Attitude Maintenance

Tables 20 and 21 are analogous to 18 and 19, the differences being that attitude control was executed by the PRCS rather than the VRCS, and the dead-bands were widened to 0.5 degrees per axis. The agreement between the results of the two programs is not as good as that previously demonstrated for VRCS control. The poorer agreement can be attributed partially to the differences in the basic PRCS force and moment tables. However, these differences are not believed great enough to explain all of the disparities between Tables 20 and 21, which probably for the most part reflect the inherent limitation of the simplified HFRMP logic when it comes to modeling the effects of the relatively high degree of overcontrol that often attends the use of the PRCS for attitude maintenance. Nevertheless, the agreement is considered adequate to satisfy the purposes of the HFRMP†, especially when taking into account the limitations of the computing equipment for which it was designed.

†i.e., relative motion studies relating to Orbiter/IUS proximity operations of comparatively short duration.

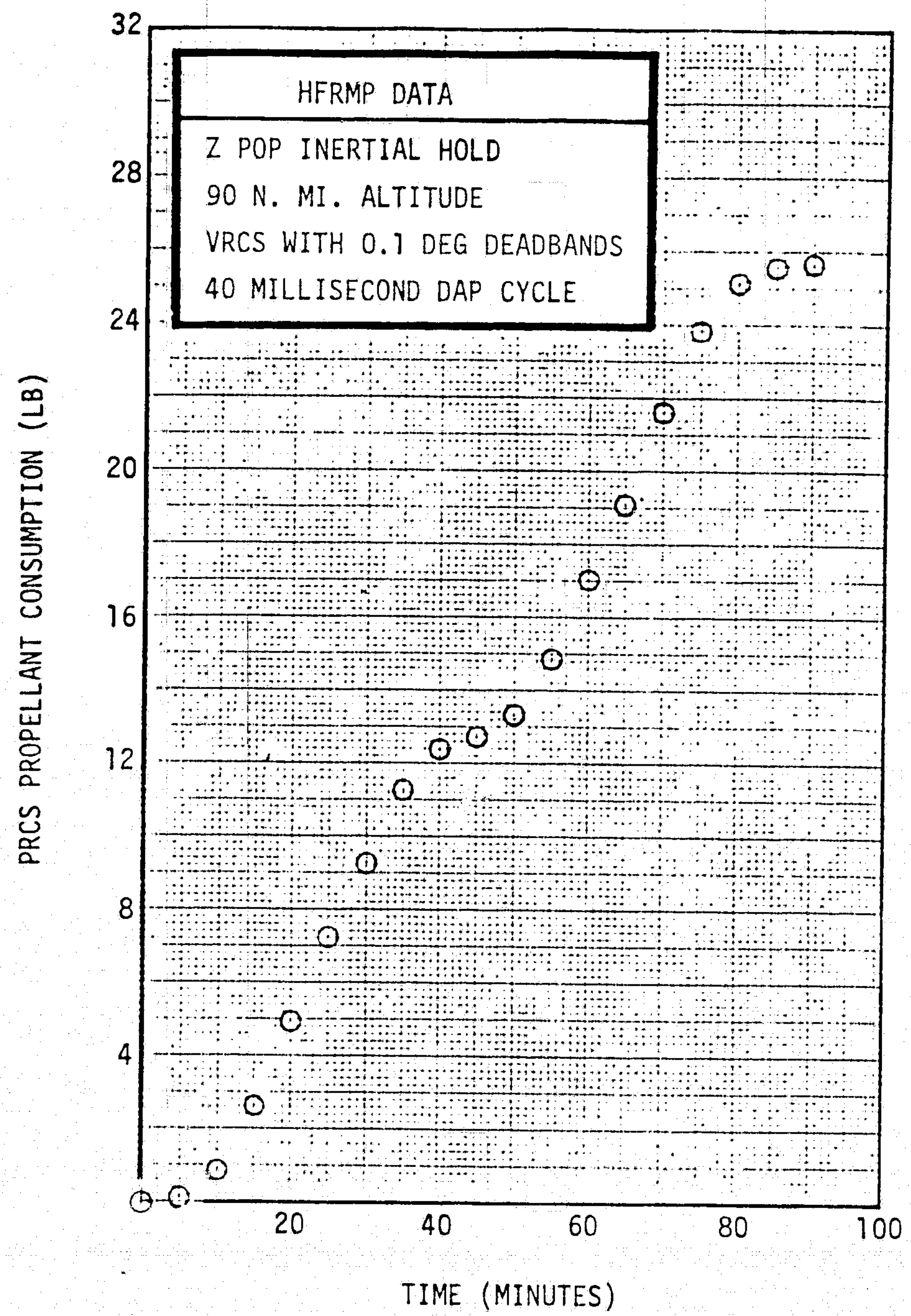

Figure 5. History of Cumulative Propellant Expenditure Over an Orbit Period

Table 20. SSFS Propellant Consumption Rates (Lb/Hr)† For PRCS Attitude Maintenance, With 40 mSec DAP Cycle

(Deadband = 0.5 Deg/Axis)

		ORBIT ALTITUDE (NAUTICAL MILES)					
		90	100	120	150	200	500
ATTITUDE	X POP INERTIAL HOLD	32	30	26	23	21	20
	Y POP INERTIAL HOLD	22	16	12	10	10	18
	Z POP INERTIAL HOLD	36	28	26	24	23	24
	X POP ZLV (HEADS DOWN)	49	38	27	23	20	14
	Y POP ZLV (HEADS DOWN)	18	18	18	18	18	17

(See Table 15 for Orbiter Mass Properties)

† - Averaged over a one-orbit period

Table 21. HFRMP Propellant Consumption Rates (Lb/Hr)† For PRCS Attitude Maintenance, With 40 mSec DAP Cycle

(Deadband = 0.5 Deg/Axis)

ATTITUDE	ORBIT ALTITUDE (NAUTICAL MILES) 90	100	120	150	200	500
X POP INERTIAL HOLD	29	26	24	24	25	26
Y POP INERTIAL HOLD	20	19	20	20	20	20
Z POP INERTIAL HOLD	28	23	18	17	17	16
X POP ZLV (HEADS DOWN)	42	34	25	25	26	27
Y POP ZLV (HEADS DOWN)	27	27	27	27	27	27

(See Table 15 for Orbiter Mass Properties)

† - Averaged over a one-orbit period

5.2 TRAJECTORY PERTURBATIONS DUE TO RCS TRANSLATIONAL CROSS COUPLING

Tables 22 and 23 contain HFRMP data relating to downtrack displacement of the Orbiter which results from uncompensated translational cross coupling during extended intervals of DAP attitude maintenance. The data were obtained by differencing the results of HFRMP runs in which ROT compensation was specified (in conjunction with both the V and the P jet select options) with similar runs in which the FULL compensation mode was specified in conjunction with the P jet select option. The displacements obtained with ROT compensation included the effects of aerodynamic drag and translational cross coupling, while the displacements obtained with FULL compensation included the effects of drag alone. Since the attitude histories were identical for all three combinations of jet-select option and compensation mode, it was reasoned that the displacements due to drag were essentially the same. It follows that when the displacements obtained with FULL compensation are subtracted from their counterparts obtained with ROT compensation, the result represents the displacement due to translational cross coupling alone.

Reference 9 contains no data of the type under consideration here. However, Reference 10 contains comparable data for two cases: Y POP ZLV at 150 miles altitude, with VRCS and PRCS control. The Reference 10 data, which were derived from SSFS simulations, are enclosed by parentheses in Tables 22 and 23. The comparisons, although severely limited in number, tend to verify the HFRMP results.

Trajectory deviations due to RCS cross coupling are of considerable import in at least two areas of on-orbit activity:

1. during stationkeeping, where they tend to drive the Orbiter away from its desired position relative to a payload, and
2. during orbit determination, where they tend to pollute navigational measurements.

By no means should the data in Tables 22 and 23 be taken as comprehensive general representations of cross coupling effects on the Orbiter's trajectory. In the first place, significant displacements can occur in directions other than downtrack. Secondly, the displacements in general are very nonlinear functions of time; therefore, the hourly "rates" shown in the cited tables

Table 22. HFRMP Downtrack Displacement Rates (Ft/Hr)[†] Due To VRCS Translational Cross Coupling, With 40 mSec DAP Cycle

(Deadband = 0.1 Deg/Axis)

		ORBIT ALTITUDE (NAUTICAL MILES)					
		90	100	120	150	200	500
ATTITUDE	X POP INERTIAL HOLD	1622	804	258	216	254	234
	Y POP INERTIAL HOLD	343	404	448	466	469	428
	Z POP INERTIAL HOLD	-149	-82	-31	-7	9	14
	X POP ZLV (HEADS DOWN)	2280	1214	447	145	45	19
	Y POP ZLV (HEADS DOWN)	34	27	23	(23)[††] 21	21	19

(See Table 15 for Orbiter Mass Properties)

† - Averaged over a one-orbit period
†† - Data from Reference 10, based on SSFS Simulation

Table 23. HFRMP Downtrack Displacement Rates (Ft/Hr)† Due To PRCS Translational Cross Coupling, With 40 mSec DAP Cycle

(Deadband = 0.5 Deg/Axis)

		ORBIT ALTITUDE (NAUTICAL MILES)					
		90	100	120	150	200	500
ATTITUDE	X POP INERTIAL HOLD	-370	-249	-216	-209	-206	-233
	Y POP INERTIAL HOLD	-150	-162	-173	-190	-224	-257
	Z POP INERTIAL HOLD	-246	-108	-24	-32	-38	-41
	X POP ZLV (HEADS DOWN)	-1137	-614	-236	-110	-82	-85
	Y POP ZLV (HEADS DOWN)	-823	-826	-830	(-744)†† -833	-837	-937

(See Table 15 for Orbiter Mass Properties)

† - Avaeraged over a one-orbit period
†† - Data from Reference 10, based on SSFS simulation

cannot be used to estimate even the downtrack displacement alone for any time interval appreciably different from the appropriate orbit period[†]. Figures 6, 7, and 8 illustrate the nonlinearity of the trajectory deviations and the diverse nature of the displacement histories for three representative attitude maintenance situations.

[†]The word "rate" is a misnomer for the data under consideration. What the tables actually represent are the displacements at the end of one orbit period, normalized to a common interval of one hour to facilitate comparisons between orbits having different periods.

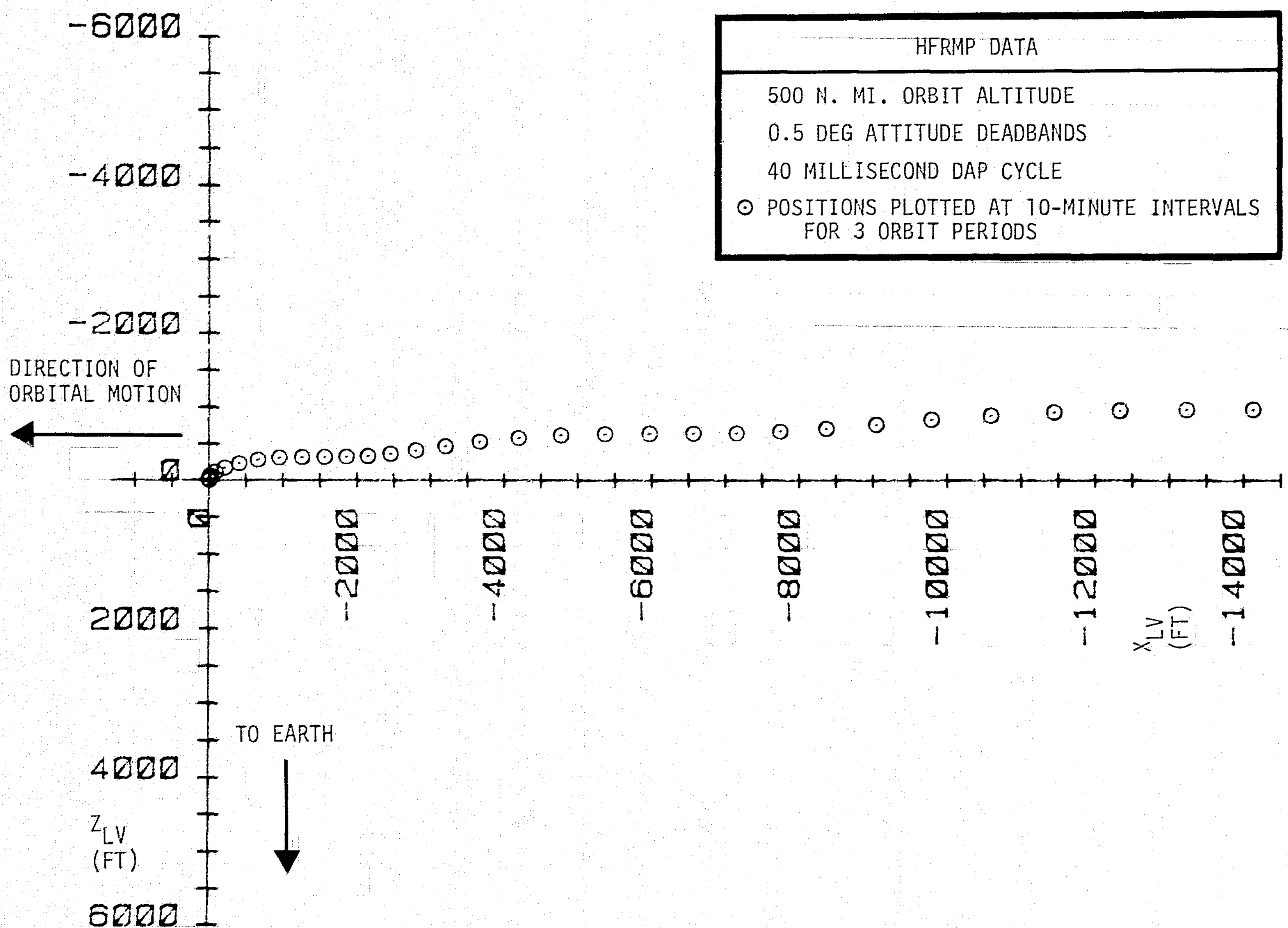

Figure 6. Orbiter Displacement Due To Cross Coupling with PRCS Holding Y POP ZLV (Heads Down) Attitude

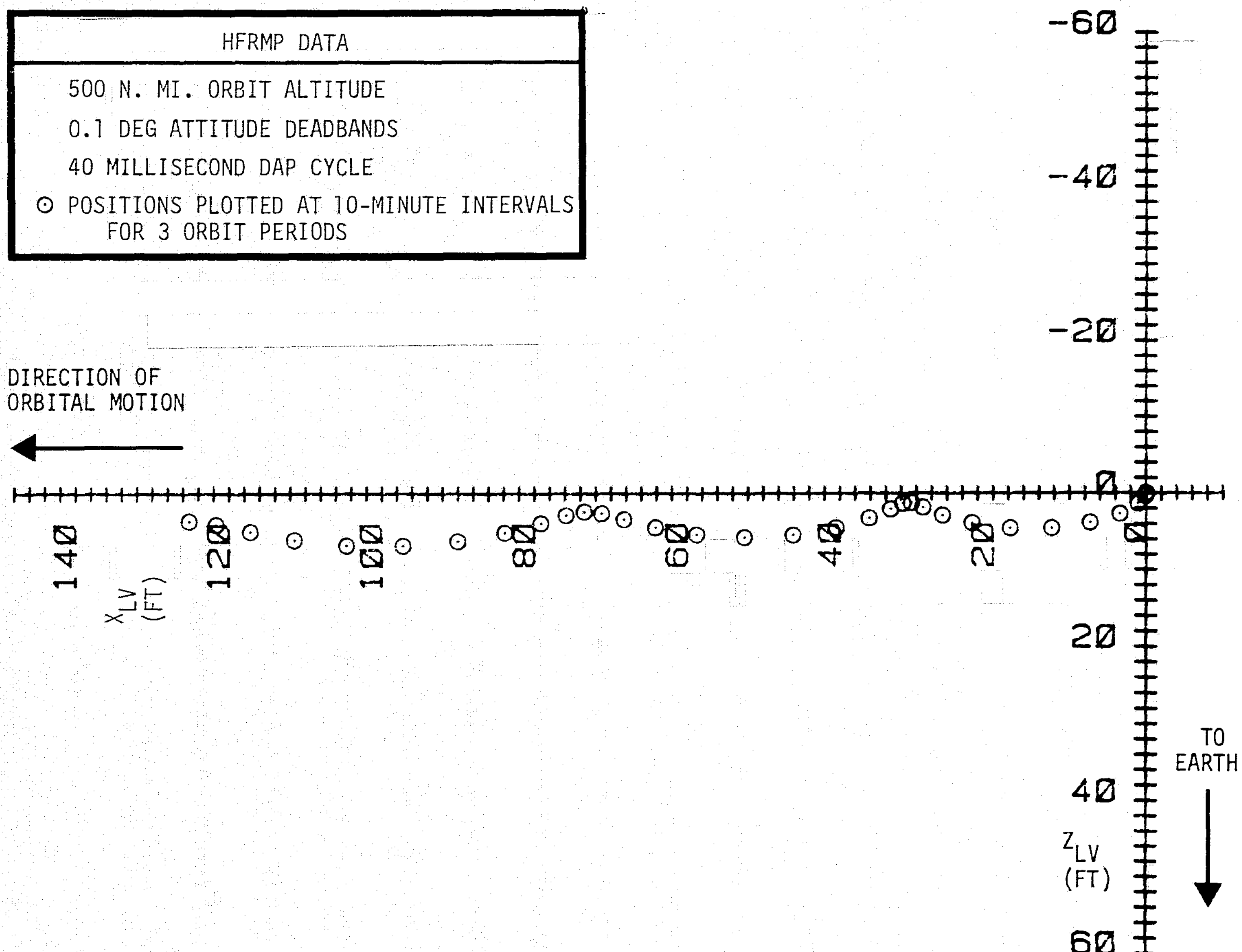

Figure 7. Orbiter Displacement Due To Cross Coupling with VRCS Holding Y POP ZLV (Heads Down) Attitude

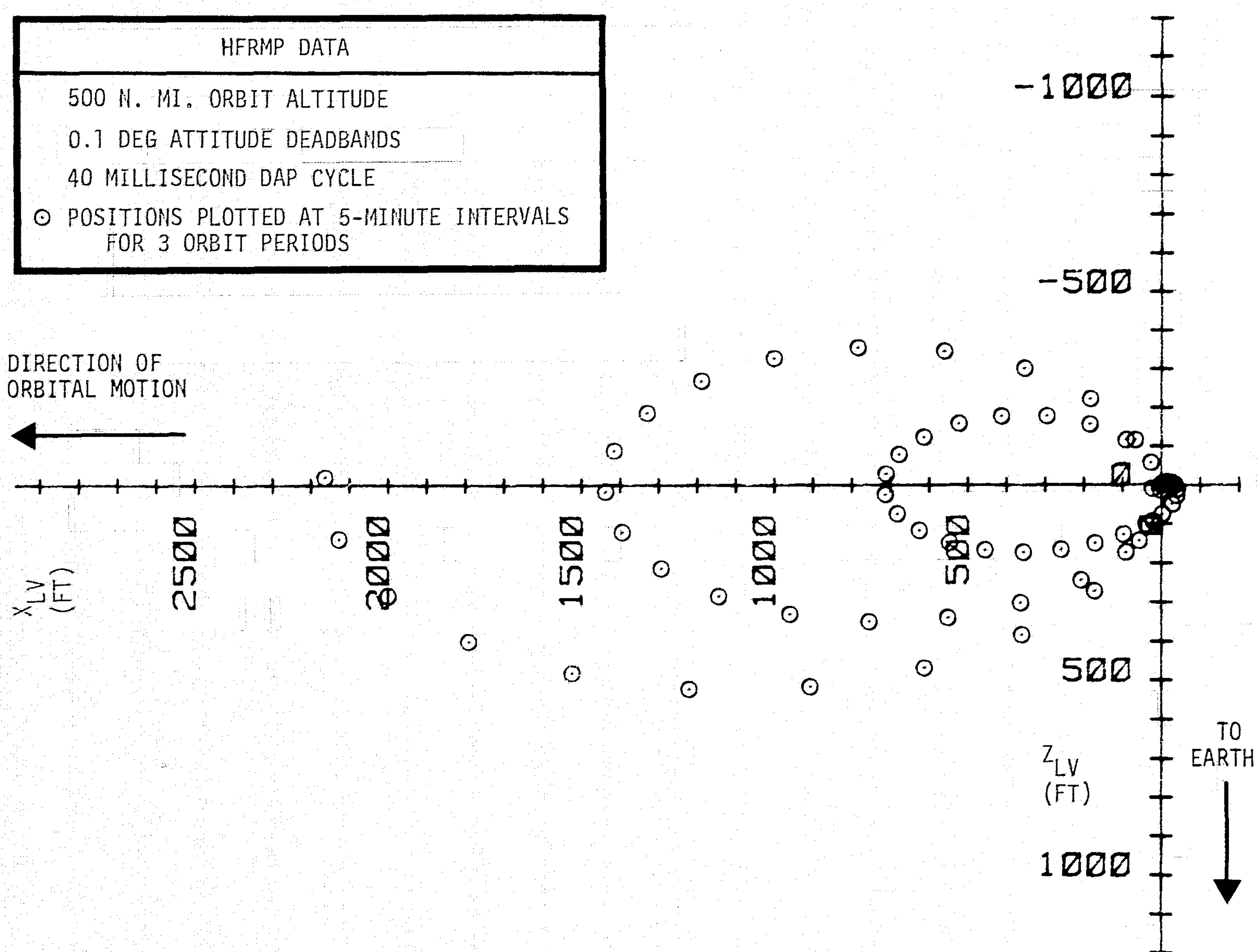

Figure 8. Orbiter Displacement Due To Cross Coupling with VRCS Holding Y POP Inertial Attitude

6. EFFECTS OF LENGTHENING THE DAP CYCLE TIME

The Shuttle DAP cycle time has recently been lengthened from the old value of 40 milliseconds to a new value of 80 milliseconds (Reference 7) to alleviate problems associated with pressure transients in the RCS propellant feed lines. This section addresses the influence of that change on trajectory perturbations and attitude-maintenance propellant requirements, as determined by the results of HFRMP calculations.

6.1 ATTITUDE MAINTENANCE PROPELLANT COSTS

Tables 24 and 25, when compared with Tables 19 and 21, indicate that the longer DAP cycle time will have a negligible effect on the VRCS propellant requirement for attitude maintenance, but that the propellant requirement for PRCS attitude maintenance within 0.5 degree deadbands will increase by as much as a factor of 5 in some cases. This result can be explained as follows. Use of the PRCS for attitude maintenance generally produces a significant degree of overcontrol (see Figure 3). In a case of extreme overcontrol, the pulse frequency is directly proportional to the minimum effective pulse width, which increases by a factor of $(.080 - .014)/(.040 - .014) \sim 2.5$ when the minimum electrical pulse width is lengthened from 40 to the new value of 80 milliseconds. The average propellant consumption rate is proportional to the product of pulse frequency and the electrical pulse width, the latter of course having been increased by a factor of $80/40 = 2$.

The preceding rationale is summarized in Equation (29), which also indicates that propellant consumption is inversely proportional to the deadband width. Therefore, if the DAP cycle time is held at 80 milliseconds, a five-fold increase in the deadband width (from 0.5 degrees to 2.5 degrees per axis) should be expected to reduce the propellant consumption rates in Table 25 to the approximate levels shown in Table 21. Table 26, which represents a four-fold increase in the deadband width, tends to support this conclusion. The same is true of Figure 9, which shows the variation of PRCS propellant consumption for deadband widths in the range of 0.5 to 10 degrees, as determined from HFRMP simulations of a representative attitude maintenance mode.

Table 24. HFRMP Propellant Consumption Rates (Lb/Hr)† For VRCS Attitude Maintenance, With 80 mSec DAP Cycle

(Deadband = 0.1 Deg/Axis)

		ORBIT ALTITUDE (NAUTICAL MILES)					
		90	100	120	150	200	500
ATTITUDE	X POP INERTIAL HOLD	14	7	3	2	2	1
	Y POP INERTIAL HOLD	3	3	3	3	3	2
	Z POP INERTIAL HOLD	17	12	8	6	6	4
	X POP ZLV (HEADS DOWN)	31	17	6	2	1	.4
	Y POP ZLV (HEADS DOWN)	.7	.6	.5	.4	.4	.3

(See Table 15 for Orbiter Mass Properties)

† - Averaged over a one-orbit period

Table 25. HFRMP Propellant Consumption Rates (Lb/Hr)† For PRCS Attitude Maintenance, With 80 mSec DAP Cycle

(Deadband = 0.5 Deg/Axis)

		ORBIT ALTITUDE (NAUTICAL MILES)					
		90	100	120	150	200	500
ATTITUDE	X POP INERTIAL HOLD	119	126	132	133	137	139
	Y POP INERTIAL HOLD	110	111	113	115	115	112
	Z POP INERTIAL HOLD	104	99	98	90	90	89
	X POP ZLV (HEADS DOWN)	126	125	134	138	139	139
	Y POP ZLV (HEADS DOWN)	139	139	139	139	139	139

(See Table 15 for Orbiter Mass Properties)

† - Averaged over a one-orbit period

Table 26. HFRMP Propellant Consumption Rates (Lb/Hr)† For PRCS Attitude Maintenance, With 80 mSec DAP Cycle

(Deadband = 2.0 Deg/Axis)

		ORBIT ALTITUDE (NAUTICAL MILES)					
		90	100	120	150	200	500
ATTITUDE	X POP INERTIAL HOLD	33	31	31	32	33	34
	Y POP INERTIAL HOLD	26	26	26	27	27	26
	Z POP INERTIAL HOLD	30	25	22	21	21	21
	X POP ZLV (HEADS DOWN)	44	37	30	33	34	34
	Y POP ZLV (HEADS DOWN)	34	34	34	34	34	35

(See Table 15 for Orbiter Mass Properties)

† - Averaged over a one-orbit period

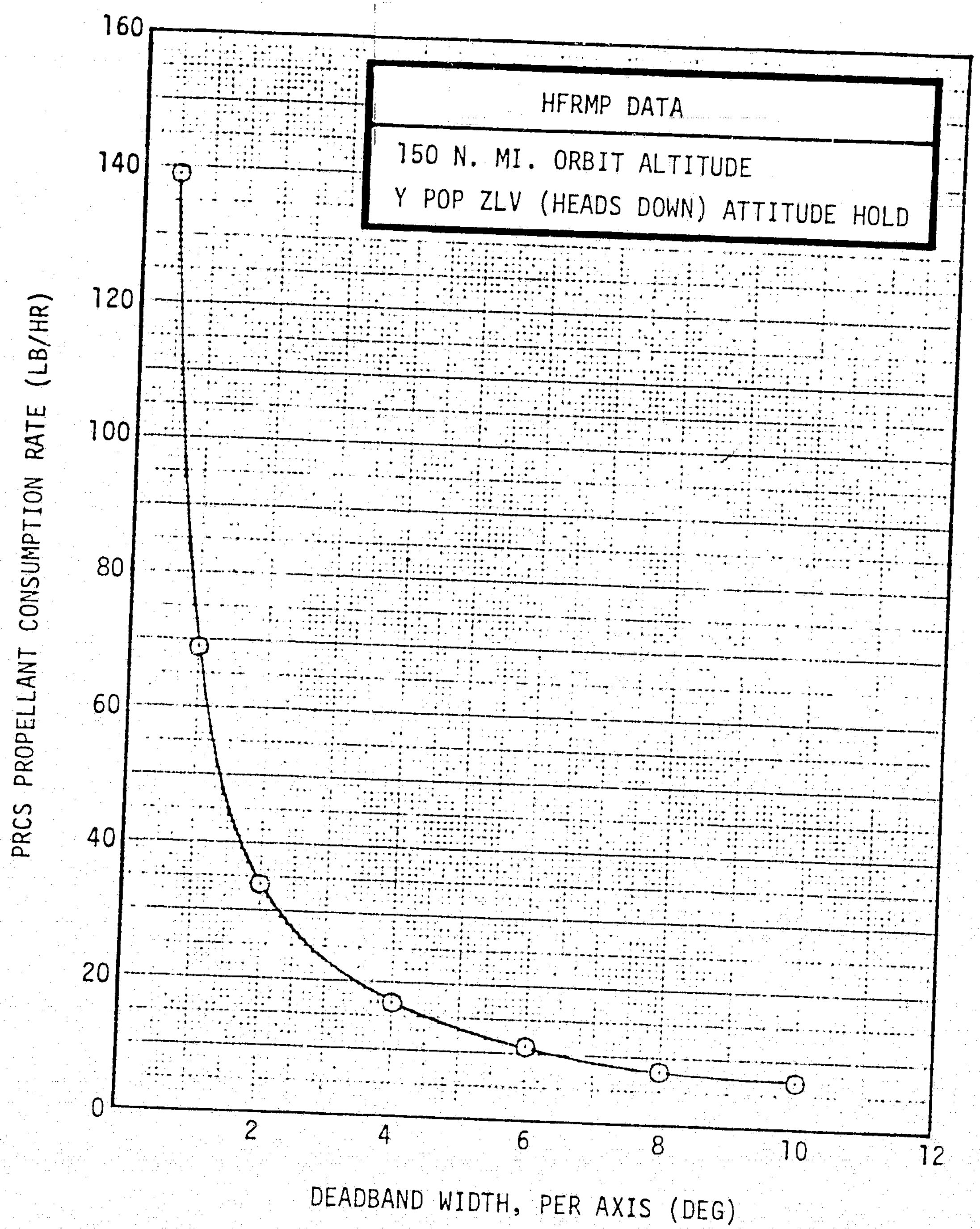

Figure 9. PRCS Propellant Consumption Rate as a Function of Deadband Width for an 80-Millisecond DAP Cycle Time

6.2 TRAJECTORY PERTURBATIONS

Table 27, when compared with Table 22, shows that the lengthened DAP cycle time has a negligible effect on the magnitude of trajectory deviations produced by translational cross coupling arising from VRCS attitude maintenance. Table 28, on the other hand, indicates (when compared with Table 23) that the corresponding effects arising out of PRCS attitude maintenance within 0.5 degree deadbands are increased by factors greater than 6. The reason that the trajectory perturbation factors are higher than the corresponding propellant consumption factors can be explained, again, in simple terms. Everything else being equal, it is logical to expect that the displacements of the Orbiter due to uncompensated cross coupling should be proportional to the total momentum content of the expelled RCS propellant, which in turn is proportional to the product of pulse frequency and the effective width of the thruster pulses (as opposed to the electrical width in the case of propellant consumption). It has already been pointed out in Section 6.1 that in a severely overcontrolled attitude maintenance situation (see Figure 3), the effective pulse width and the pulse frequency are each increased by a factor of approximately 2.5 when the DAP cycle time is increased from 40 to 80 milliseconds. Therefore, in this kind of situation, the trajectory deviations should be expected to increase by a factor of approximately $(2.5)^2 = 6.25$.

As indicated by Table 29, the effect of the lengthened DAP cycle on Orbiter trajectory perturbations can be ameliorated by increasing the attitude deadband width, in the same manner (and in the same proportion) as it can be in the case of propellant consumption; provided of course that other operational considerations will permit the use of the wider deadbands.

Significant increases in the attitude deadband widths may not be feasible, for instance, when the Orbiter is stationkeeping at close range with a free-flying payload. In such a case, precise translational control of the Orbiter must be maintained by the pilot on the basis of the visually observed relative motion of the payload. In the presence of large Orbiter attitude excursions, it is difficult for the pilot to determine whether a change in the apparent position of the payload is actually due to relative translational motion, or

Table 27. HFRMP Downtrack Displacement Rates (Ft/Hr)† Due To VRCS Translational Cross Coupling, With 80 mSec DAP Cycle

(Deadband = 0.1 Deg/Axis)

	ORBIT ALTITUDE (NAUTICAL MILES)					
ATTITUDE	90	100	120	150	200	500
X POP INERTIAL HOLD	1622	804	258	216	257	238
Y POP INERTIAL HOLD	343	405	449	469	478	440
Z POP INERTIAL HOLD	-149	-82	-31	-7	9	14
X POP ZLV (HEADS DOWN)	2280	1214	447	145	45	23
Y POP ZLV (HEADS DOWN)	34	28	24	23	23	22

(See Table 15 for Orbiter Mass Properties)

† - Averaged over a one-orbit period

Table 28. HFRMP Downtrack Displacement Rates (Ft/Hr)[÷] Due To PRCS Translational Cross Coupling, With 80 mSec DAP Cycle

(Deadband = 0.5 Deg/Axis)

		ORBIT ALTITUDE (NAUTICAL MILES)					
		90	100	120	150	200	500
ATTITUDE	X POP INERTIAL HOLD	-1199	-1247	-1302	-1328	-1365	-1547
	Y POP INERTIAL HOLD	-864	-881	-889	-960	-1187	-1468
	Z POP INERTIAL HOLD	166	272	200	-95	-221	-269
	X POP ZLV (HEADS DOWN)	-1254	-808	-569	-484	-471	-528
	Y POP ZLV (HEADS DOWN)	-5516	-5512	-5517	-5528	-5544	-6173

(See Table 15 for Orbiter Mass Properties)

÷ - Averaged over a one-orbit period

Table 29. HFRMP Downtrack Displacement Rates (Ft/Hr)† Due To PRCS Translational Cross Coupling, With 80 mSec DAP Cycle

(Deadband = 2.0 Deg/Axis)

		ORBIT ALTITUDE (NAUTICAL MILES)					
		90	100	120	150	200	500
ATTITUDE	X POP INERTIAL HOLD	-424	-330	-334	-334	-337	-381
	Y POP INERTIAL HOLD	-239	-245	-247	-265	-320	-385
	Z POP INERTIAL HOLD	-209	-70	-2	-39	-58	-66
	X POP ZLV (HEADS DOWN)	-1146	-628	-249	-152	-126	-134
	Y POP ZLV (HEADS DOWN)	-1350	-1352	-1356	-1360	-1365	-1525

(See Table 15 for Orbiter Mass Properties)

† - Averaged over a one-orbit period

due to a rotation of his reference frame (the Orbiter)*. On the other hand, if the attitude deadbands are not widened, the lengthened DAP cycle may require the pilot to execute manual translational corrections much more frequently to compensate for the greater translational deviations which attend the automatic maintenance of attitude by the DAP. As illustrated in Figures 10 and 11, this is especially true if it is necessary to inhibit the upward-firing (+Z) PRCS jets to minimize plume impingement effects on the payload.

It is not the intent of this discussion to attempt a general evaluation of the overall influence of the lengthened DAP cycle on Orbiter/payload proximity operations. Such an evaluation is far beyond the scope of this report, not to mention the limited capabilities of the HFRMP computer program. The intent is rather to point out and to describe some potential operational problems that are suggested by results obtained from the relatively simplified HFRMP calculations, and which would seem to merit a more comprehensive investigation involving a real-time man-in-the-loop simulator.

In this vein, one final observation will be made; this time with regard to the potential influence of the lengthened DAP cycle time on the dynamic effects of Orbiter RCS plume impingement on a nearby payload. Even when special precautions are taken to fire only those RCS thrusters whose plume centerlines extend away from or at right angles to the payload, the plumes expand sufficiently to cause sensible perturbations of the payload attitude in many cases. Again assuming everything else to be equal, the magnitude of these perturbations can be expected to increase in direct proportion to the total momentum content of the expelled RCS propellant. For a given Orbiter deadband, it follows then that the lengthened DAP cycle should increase payload attitude perturbations in the same ratio as that previously calculated for Orbiter translational perturbations, i.e., by a factor of approximately 6.25.

---

*In some cases, such as in a grappling operation, this makes little difference since any kind of relative motion (whether its origin is rotational or translational) is objectionable.

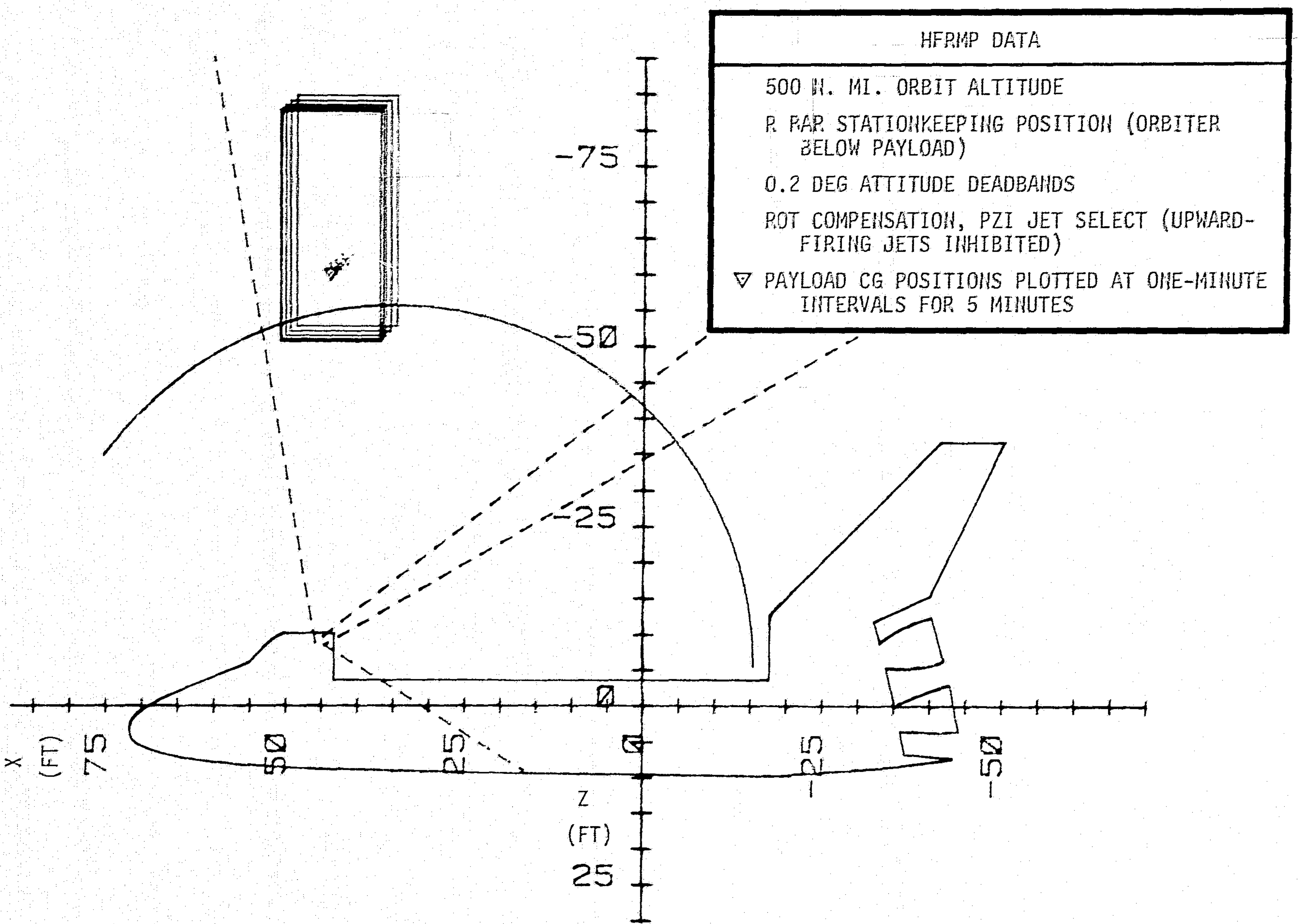

Figure 10. Hands-Off Stationkeeping Errors with 40 Millisecond DAP Cycle

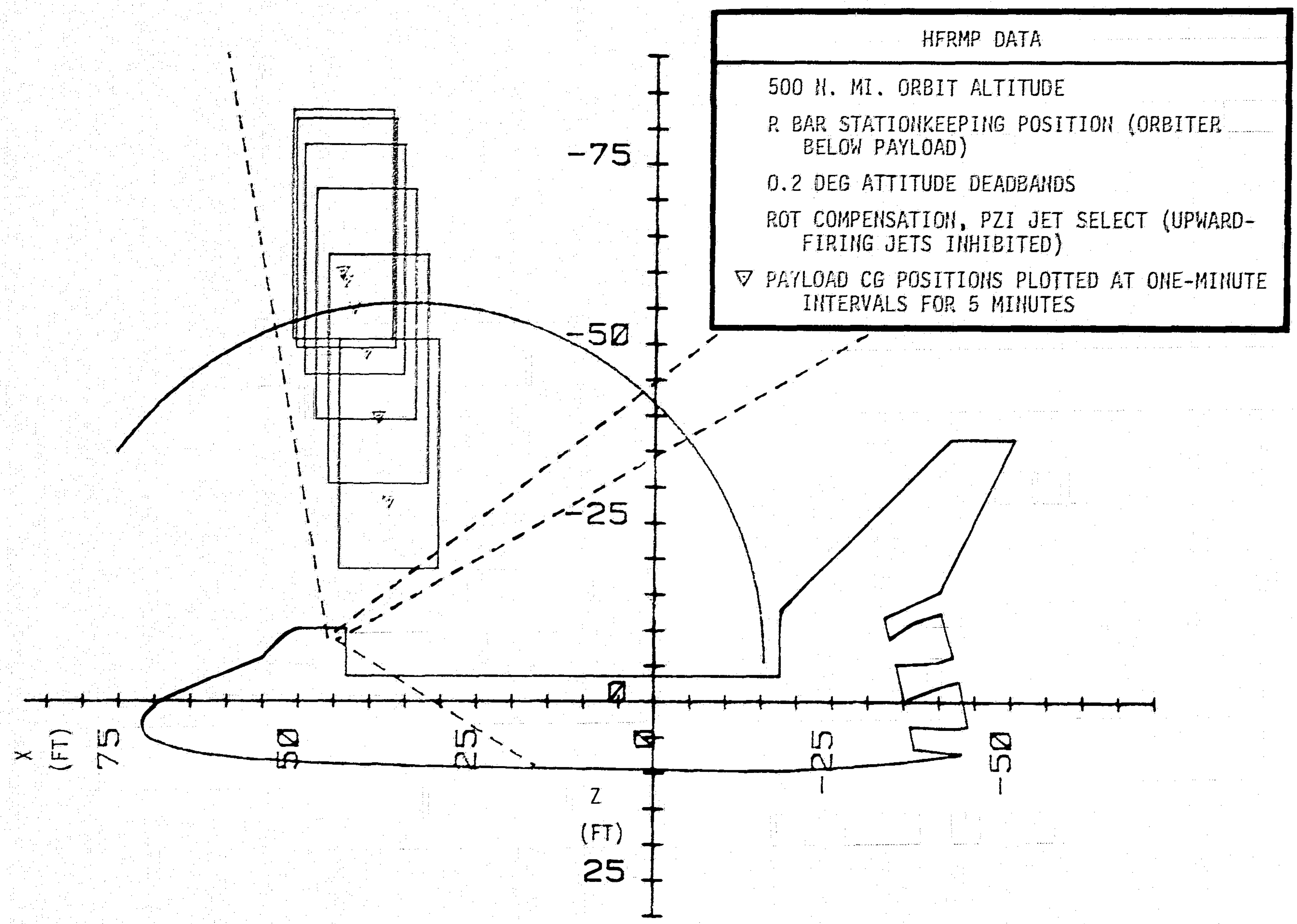

Figure 11. Hands-Off Stationkeeping Errors with 80 Millisecond DAP Cycle

7. CONCLUSIONS AND RECOMMENDATIONS

Comparisons of data generated by the HFRMP and the SSFS computer program (Section 5) fail to indicate any gross errors in the HFRMP models of the Orbiter OMS/RCS/DAP system. On the basis of these comparisons, it is believed that the HFRMP models are sufficiently accurate to produce valid flight profile designs for proximity operations flight phases.

The absolute accuracy of the simplified HFRMP attitude control logic could not be established for PRCS maneuvers and attitude maintenance because the published SSFS data which are currently available were generated prior to certain revisions of the PRCS thruster force and moment tables that were incorporated in the HFRMP data base. Recent inquiries directed to personnel familiar with the SSFS indicate that the PRCS forces and moments currently used by that program are still somewhat different from those used in the HFRMP, by reason of differences in the plume impingement effects which are presented in Table 3. These inquiries revealed also that a revision of the plume impingement data is expected in the near future. With this in mind, it was decided to postpone any effort toward a more precise correlation of HFRMP and SSFS data. However, after the plume impingement updates become available and have been incorporated in both programs, further data comparisons are recommended for the purpose of establishing the accuracy of the HFRMP models more firmly.

It is believed that the simplified RCS/DAP models utilized in the HFRMP are potentially useful in connection with ground-based orbit determination, where they might be used to estimate trajectory deviations attributable to RCS cross coupling (see Figures 6, 7, and 8).

Finally, the potential close-range stationkeeping problems that are suggested by the HFRMP simulations of 80 millisecond DAP cycle effects (Section 6) are believed to be of sufficient import to merit further investigation by means of a real-time man-in-the-loop simulator; preferably one which models the dynamic effects of RCS jet plume impingement on the payload.